AIAA Guidance, Navigation, and Control Conference
08 - 11 August 2011, Portland, Oregon

AIAA 2011-6615

Extended Kalman Filter vs. Error State Kalman Filter for Aircraft Attitude Estimation

Venkatesh K. Madyastha*
Flight Mechanics & Control Division, National Aerospace Laboratories, Bangalore, 560017, India.

Vishal C. Ravindra†
Flight Mechanics & Control Division, National Aerospace Laboratories, Bangalore, 560017, India.

Srinath Mallikarjunan‡
Unmanned Dynamics, Chennai, 600006, India.

Anup Goyal§
Flight Mechanics & Control Division, National Aerospace Laboratories, Bangalore, 560017, India.

The Kalman filter (KF) is the optimal estimator that minimizes the mean square error when the state and measurement dynamics are linear in nature, provided the process and measurement noise processes are modeled as white Gaussian. However, in the real world, one encounters a large number of scenarios where either the process or measurement model (or both) are nonlinear. In such cases a class of suboptimal Kalman filter implementations called extended Kalman filters (EKF) are used. EKFs operate by linearizing the nonlinear model around the current reference trajectory and then designing the Kalman filter gain for the linearized model. Recently, an alternative approach has emerged for a certain class of problems where the *error in the states* is estimated using a Kalman filter, rather than the state itself. This error state KF (ErKF) approach, by deriving the error state dynamics, via the perturbation of the nonlinear plant, lends itself to optimal updates in the error states and optimal prediction and updates in the error state covariance. This is because the error state dynamics are linear, thereby satisfying a condition for optimal Kalman filtering. This paper offers a comparison between the EKF and ErKF via simulations and shows that the ErKF performance is robust to a variety of aircraft maneuvers performed. Furthermore, this paper shows that the ErKF, unlike the EKF, need not be repeatedly tuned with respect to the noise covariances in order to obtain acceptable estimation performance.

I. Introduction

The availability of direct measurements for all state variables is a rare occasion in practice. In physical systems, some components of the state vector are inaccessible internal variables, which either cannot be measured or the measurements require the use of very costly measurement devices. Therefore, it is either not feasible or it is very expensive to measure all the state variables. Hence, in most practical scenarios there is a true need to construct estimates of the unknown state variables via known measurements.

For the case of linear dynamical systems with deterministic disturbances, the Luenberger observer offers a complete and comprehensive answer to the problem of state estimation.[1] In the case of systems that are linear in the process and measurement, and which are exogenously corrupted by white process noise and measurement noise, some of the early methods for observer design, which date as far back as the early

*Scientist Fellow, Flight Mechanics & Control Division, National Aerospace Laboratories. Email: vmadyastha@nal.res.in or venky107@gmail.com

†Scientist Fellow, Flight Mechanics & Control Division, National Aerospace Laboratories. Email: vishalcr@nal.res.in or vishalcr@gmail.com

‡Scientist, Unmanned Dynamics. Email: srinath@unmanned-dynamics.com or srinath3142@gmail.com

§Scientist Fellow, Flight Mechanics & Control Division, National Aerospace Laboratories. Email: anup.goyal0@gmail.com

1940's, involved the Wiener-Hopf filter, which is a linear system[2,3] and the Kalman-Bucy filter,[4–6] which is a model-based filtering approach. The major contribution of the Wiener filter to observer theory was in the derivation of the steady state optimal filter and predictor for stochastic stationary scalar processes using spectral factorization techniques. On the other hand, in the development of the Kalman filtering theory, the input-output signal Wiener model was replaced by a state-space model, and a recursive solution of the optimal state estimator was obtained for stationary and non stationary cases. Furthermore, the Kalman filter offers a recursive solution in the sense of minimizing the trace of the error covariance of the system states. In other words, the Kalman filter can also be called as a minimum variance estimator. The Wiener and Kalman filters are optimal filters in the least squares sense and are equivalent to each other in steady state.[7] In the aforementioned filter designs it is assumed that the spectral properties of the signal and noise processes in the case of the Wiener filter, and the covariance matrices of the process and measurement are completely known. A typical time invariant linear system in discrete time is represented as

$$\begin{aligned} \xi_{k+1} &= A\xi_k + Bu_k + Gw_k, \qquad \xi(0) = \xi_0 \\ z_k &= C\xi_k + v_k \end{aligned} \tag{1}$$

where ξ_k denotes the vector of the system states, u_k denotes the vector of the system inputs, w_k denotes the vector of the process noise, z_k denotes the vector of the system outputs, v_k denotes the vector of the measurement noise, A denotes the system state matrix, B denotes the system input matrix, G denotes the process disturbance matrix, C denotes the output/measurement matrix and ξ_0 denotes the initial value of the system states. One of the major advantages of using the Kalman filter (KF) is its ability to predict and update the states recursively, making it ideal for online application. *It should be noted that all the states of the system need not be measured in order to estimate them.* The philosophy of the KF is to use available measurements in order to estimate even those states that are not necessarily measured. However, in the case of systems which are inherently nonlinear in either the process dynamics or the measurement or both, straightforward implementation of the linear KF is not guaranteed to yield optimum results in the sense of minimizing the root mean square of the estimation error. Thus the need to be able to effectively reconstruct the unknown states of a nonlinear system has promoted research in nonlinear filtering theory.

The design of nonlinear filters is a very challenging problem and has received a considerable amount of attention in the literature over the past few decades.[8,9] A typical time invariant nonlinear system in discrete time can be represented as

$$\begin{aligned} \xi_{k+1} &= f\left(\xi_k, u_k, w_k\right), \qquad \xi(0) = \xi_0 \\ z_k &= h\left(\xi_k\right) + v_k \end{aligned} \tag{2}$$

where, as before, ξ_k denotes the vector of the system states of the nonlinear system in Eq. (2), u_k denotes the vector of the system inputs, w_k denotes the vector of the process disturbances, z_k denotes the vector of the system outputs, v_k denotes the vector of the measurement disturbances, $f\left(\cdot,\cdot,\cdot\right)$ denotes the nonlinear process function that maps the system states, inputs and disturbances to the state derivatives (dynamics), $h\left(\cdot\right)$ denotes the measurement nonlinear function of the system states and ξ_0 denotes the initial value of the system states. The process and measurement noise processes have zero mean and prescribed covariances, which are commonly denoted in the literature as Q_k and R_k respectively. Of the numerous attempts being made for the development of nonlinear filters, the extended Kalman filter (EKF) is the most popular approach[a]. The design of the EKF is typically based on a first order local linearization of the system around a reference trajectory at each time step.[6,10–12] Thus the partial derivative of the nonlinear system dynamics is computed with respect to the system states and evaluated at the state estimate for each time step. The EKF is an estimator that handles nonlinearities in the dynamical processes as well as measurements and furthermore, akin to a KF, treats systems with the process and measurement dynamics corrupted by white Gaussian noise. The EKF[11,13–15] was conceptualized as an engineering approximation to a difficult theoretical problem. The issue was about estimating the state of a nonlinear system from available measurements in the presence of disturbances. Since their inception, EKFs have been successfully applied for the purpose of state estimation for nonlinear stochastic systems.[16–18] In the case of systems that have absolutely no noise in either the process or the measurement, i.e., perfect model and noise free sensor(s), the EKF can be designed to function as a state estimator for a deterministic nonlinear system.[19] The results in[19] have been strongly motivated by some large deviation results for certain conditional measures as reported in.[20]

[a]EKF is a class of approaches that approximates the problem and then applies linear Kalman filtering techniques.[9]

The objective in[19] is to describe a design procedure for constructing an observer for a noise free nonlinear dynamical system which forms the limiting solution for a noisy nonlinear dynamical system. A limiting parameter is associated with the process as well as measurement noise vectors and as this limiting parameter approaches 0, the behavior of the observer for the noisy system approaches the behavior of an observer for a noise free deterministic system. The stability and convergence properties of EKFs have been a subject of research for over a decade now. In,[21] it is shown that the EKF is guaranteed to be a nondivergent estimator[b] A nondivergent estimator can be used to create a model-based nonlinear control system without loss of stability when the estimated state is substituted for the actual state in a stabilizing state-feedback function. The conditions which guarantee that the EKF will be nondivergent are roughly that the nonlinearities have bounded slope, the inputs enter additively, and the system is M-detectable[c] In the research reported in,[19] an asymptotic limit of a stochastic filter is arrived at through the efficient construction of a deterministic observer. Literature study suggests that while EKFs show exponentially convergence behavior for a general class of systems, these results are still local in nature as has been reported in.[22–24,26,27] In,[22] a connection is shown between the appropriate choice of Q_k and R_k and the usefulness of the EKF. A linearization technique as developed in,[23] which consists of introducing unknown diagonal matrices to take the approximation errors into account, is used. The problem of showing stability results is recast into a linear matrix inequality problem, which in turn establishes the connection between a good convergence behavior of the EKF and the covariance matrices Q_k and R_k. In,[26] an EKF is designed with an *a priori* prescribed degree of stability. The equilibrium point of the EKF error dynamics is shown to be an exponentially stable equilibrium point. A critical assumption to establishing the results in[26] is that the norm of the higher order Taylor series terms are proportionally upper bounded by the square of the error terms. This assumption aids in showing that the EKF is an exponential observer. Furthermore, in[22] and,[26] the domain of attraction of the EKF has been studied in detail. One suggestion is to set the Q_k matrix sufficiently large so that the EKF can tolerate arbitrarily large errors in the initialization of the state estimation errors. In,[24] the authors establish stability results for continuous-continuous (process and measurement are continuous) and continuous-discrete (process is continuous while the measurement is discrete) EKFs derived from the observer of.[28] The authors of[24] show that so long as the noise covariance matrices (Q_k and R_k) are properly parameterized, the EKF takes the form of a *time-varying high-gain* observer that asymptotically approaches a fixed gain observer as the gain is increased. Furthermore, in[24] it is shown that under conditions of the Lie derivatives of the measurement forming a diffeomorphism[d] and a global Lipschitz property on the system nonlinearities, the EKF is a global exponential observer for a class of nonlinear systems which are transformable to a lower triangular form. In,[29] an observer-based control structure for a standard nonlinear model of polymerization reactors is proposed using a classical input/output linearization technique for the controller design and guaranteeing global asymptotic closed-loop stability. The unknown states which are estimated via an exponentially convergent observer, similar to the equations of an EKF, are used to form the control law. In,[30] it is shown that despite restrictive assumptions on the nonlinearities and exponential stability of the estimation error, does not guarantee the behavior of the closed-loop system, even when the system under state feedback is exponentially stable. Thus there has been a strong research effort to analyze the behavior of a closed-loop system with an estimator such as an EKF is used as an observer. Toward this end,[18] relaxes the global Lipschitz condition and considers a class of systems transformable to the special normal form with linear internal dynamics. The closed-loop system with the EKF is then represented in the standard singularity perturbed form via a parameterization of the Riccati equation. Furthermore, by relaxing the global Lipschitz condition, difficulties may arise as a result of the peaking phenomenon,[33] which can lead to instability in the closed-loop system. Peaking phenomenon occurs when high-gain feedback is used to produce eigenvalues with very negative real parts whereby some states peak to very large values, before rapidly decaying to zero. This phenomenon is typically overcome by globally bounding the control outside a compact region of interest. Many successful applications of the EKF are described in[32,34] and other areas such as monitoring of membrane bioreactor systems,[35–37] adaptive state estimation, nonlinear estimation,[38] parameter estimation, target tracking, training of neural networks, formation flying,[39,40] ballistic projectile state estimation,[41–43] navigation in unknown terrain environments,[44,45] etc.

[b] A nondivergent estimator[15] is one for which the size of the estimation error is no more than proportional to the size of the process noise and the measurement noise.

[c] A system is M-detectable[15] if a model-based estimator exists that is nondivergent for a full rank input matrix (not necessarily the output matrix).

[d] A diffeomorphism is an invertible function that maps one differentiable manifold to another, such that both the function and its inverse are smooth.[25]

"Engineers can solve exact problems using numerical approximations, or they can solve approximate problems exactly" - Fred Daum.[9] The procedure of linearizing the nonlinear dynamics and/or nonlinear measurement equations that occur in practical problems and computing the Kalman gain based on the linearized equations is the philosophy of an EKF. In contrast, error state Kalman filter described in[46,47] solves an approximate problem with exact solutions by recasting the problem from state domain to error-state domain.

The error state Kalman filter (ErKF) was introduced in[46] for a mobile robot localization problem. In this problem, as well as in general autonomous navigation problems, the accurate estimation of position and attitude is essential for the guidance and control algorithms to perform effectively. Internal sensors (mounted on ownship) such as gyroscopes, accelerometers and magnetometers are used to provide measurements of instantaneous angular velocities, specific forces and heading, respectively.[47,48] External sensors such as the global positioning system (GPS) provide measurements of the position, velocity and track angles of the vehicle. Often times the measurements from various sensors are fused in order to enhance the quality of the estimates.[47,48] However, the most basic forms of navigation rely on internally mounted sensors or so called "strapdown" inertial sensors.[48] Inertial navigation systems (INS) are widely used in air vehicle navigation and outdoor robotics.[46,49] The suite of sensors that constitute an INS is called an inertial measurement unit (IMU), and it typically consists of gryoscopes that measure the angular velocity and accelerometers that measure the specific force in the body axis of the vehicle. The INS calculates via dead reckoning the estimates of the orientation, position and velocity. It accomplishes this by integrating the rigid body kinematic equations of the angular velocity and acceleration using known initial orientation and velocity, respectively, to obtain the orientation (attitude) estimates and velocity estimates, and by integrating the velocity equations to obtain the position estimates, given a known initial position.

It is a known fact that inertial sensors suffer from biases as well as stochastic errors that need to be modeled.[47] A classical INS integrates the measurements provided by the sensors in the IMU to obtain attitude as well as position and velocity estimates. Hence, the error in the calculation of attitude, position and velocity grows unbounded with time if not periodically reset or without aiding using external measurements. Kalman filter based algorithms have been used for estimation of the absolute states such as attitude, position and velocity, as well as the biases and other error parameters. For the attitude estimation problem, there two classes of (process) modeling used: dynamic or vehicle specific modeling and strapdown modeling. The attitude kinematics represented via Euler angles is given by[48,50,51]

$$\begin{bmatrix} \dot{\psi} \\ \dot{\theta} \\ \dot{\phi} \end{bmatrix} = \frac{1}{\cos\theta} \begin{bmatrix} 0 & \sin\phi & \cos\phi \\ 0 & \cos\phi\cos\theta & -\sin\phi\cos\theta \\ \cos\theta & \sin\phi\sin\theta & \cos\phi\sin\theta \end{bmatrix} \begin{bmatrix} p \\ q \\ r \end{bmatrix} \tag{3}$$

where ψ, θ and ϕ are the yaw, pitch and roll angles, and p, q and r are the angular velocities or the rates measured by rate gyros. The attitude can be obtained by the integration of Eq. (3) if the initial attitude is known. In[52] the so-called dynamic modeling approach is adopted whereby the angular rates are included in the state vector to be estimated and the rates measured by the gyros are used as measurements by the KF. In a strapdown model, as adopted in,[46–48,50,51] the *errors in the attitude* rather than attitude itself are included in the state vector, while the attitudes measured by an aiding sensor are used as measurements. However, the so-called dynamic modeling approach (it has also been called the direct filtering approach in[46]) has the following drawbacks:[46,51] (a) the dynamic model is dependent on the vehicle, so every time a modification is made, or a part is relocated, or its mass changes, etc., the dynamic modeling has to be altered, (b) dynamic modeling would require a larger number of states and the knowledge of the vehicle motion parameters, and (c) precise modeling of the interaction of the platform and the environment is required. In[46,51] an error-state filter is derived where the errors in attitude are included in the state vector, while the error propagation equations are derived from the strapdown equations given in Eq. (3) that contains the gyro measurements. In the error-state formulation, the Euler angles are obtained via integration of the plant given in Eq. (3), while the estimated errors are fed-back into the Euler angles at each time step. The bias in gyro measurements can also be included in the state vector and can be fed back to the plant at each time step. The measurements used in the KF for the error state formulation are the attitude measurements obtained via other aiding sensors such as the accelerometer and the magnetometer. Some successful applications of the ErKF are described in.[47,50,71] In the research reported in,[71] a simultaneous localization and mapping (SLAM)[e] algorithm is developed using vision sensors for navigation in unknown, urban environments where

[e]A SLAM algorithm is a landmark based terrain aided navigation system (TANS) that has the capability to build online

global positioning system (GPS) outages are a frequent phenomenon, or where GPS signals are not available.

One of the inherent limitations of the EKF is in re-tuning of the noise covariance matrices, Q_k and R_k, and the initial state error covariance matrix, to suit the particular regime of vehicle operation.[53–55] It is a well known fact that the uncertainty of these covariance matrices has an impact on the performance of the EKF. Any uncertainty in these covariance matrices, due to improper tuning, can have an adverse effect on the filter and at times might even cause it to diverge. In a conventional setting, the determination of the noise covariance matrices requires a good knowledge of the process and the measurement model. In this paper, we propose to compare the performances of the EKF and the ErKF for a suite of aircraft maneuvers without re-tuning the noise as well as the state error covariances matrices. Thus, once these covariance matrices have been tuned as per the process and sensor specifications, they should not be re-tuned when different flight conditions are encountered such as presence or absence of turbulence or when different aircraft maneuvers are performed for which the covariances are not necessarily optimal. To the best of our knowledge, this kind of a filter performance comparison of an ErKF against a conventional EKF has not been attempted yet. Furthermore, this paper attempts to point out, via the problem formulation and filter design, some of the differences between the EKF and the ErKF. The rest of the paper is structured as follows: Section II provides a mathematical formulation of problem considered and a framework for designing the EKF and the ErKF. In Section III, a typical attitude heading reference system problem is formulated for aircraft attitude estimation with measurements from sensors such as gyroscopes and accelerometers. Section IV presents some simulations for the problem developed in Section III for a suite of different aircraft maneuvers. Furthermore, we present an important remark (Remark IV.1) in Section IV which forms the basis for this paper. The performance of an EKF and an ErKF are compared and contrasted for all these maneuvers. Finally, Section V contains some concluding remarks and some future plans. Throughout the paper, bold symbols are used for vectors, capital letters for matrices and small letters for scalars.

II. Generic Problem Formulation

Consider a nonlinear, bounded, observable[f] system with continuous process dynamics and discrete measurement as

$$\begin{aligned} \dot{\mathbf{x}}(t) &= \mathbf{f}(\mathbf{x}(t), \mathbf{u}(t)) + \Gamma \mathbf{w}(t), \qquad \mathbf{x}(0) = \mathbf{x}_0 \\ \mathbf{z}_k &= \mathbf{h}(\mathbf{x}_k) + \mathbf{v}_k \end{aligned} \tag{4}$$

where, $\mathbf{x} \in \mathcal{D}_{\mathbf{x}} \subset \mathcal{R}^n$ denotes the $n-$dimensional state vector of the system, $\mathbf{u} \in \mathcal{D}_{\mathbf{u}} \subset \mathcal{R}^m$ denotes the $m-$dimensional known input vector, $\mathbf{w} \in \mathcal{D}_{\mathbf{w}} \subset \mathcal{R}^{n_w}$ denotes the n_w-dimensional random process noise, $\mathbf{z}_k \in \mathcal{D}_{\mathbf{z}} \subset \mathcal{R}^p$ denotes the $p-$dimensional system measurement, $\mathbf{v}_k \in \mathcal{D}_{\mathbf{v}} \subset \mathcal{R}^p$ denotes the $p-$dimensional random measurement noise, $\mathbf{f}(\cdot,\cdot) : (\mathcal{D}_{\mathbf{x}} \subset \mathcal{R}^n) \times (\mathcal{D}_{\mathbf{u}} \subset \mathcal{R}^m) \to \mathcal{R}^n$ is a finite nonlinear mapping of the system states, $\mathbf{h}(\cdot) : \mathcal{D}_{\mathbf{x}} \subset \mathcal{R}^n \to \mathcal{R}^p$ is a nonlinear mapping of the system states and $\Gamma \in \mathcal{R}^{n \times n_w}$ is the process noise scaling matrix. The process and measurement noise are assumed to be zero mean, band-limited, uncorrelated, white multivariate Gaussian processes given by

$$\begin{aligned} E\left[\mathbf{w}(t)\,\mathbf{w}^T(\tau)\right] &= Q\delta(t-\tau) = \begin{cases} Q, & t = \tau \\ 0, & t \neq \tau \end{cases} \\ E\left[\mathbf{v}_k \mathbf{v}_j^T\right] &= R_k \delta_{kj} = \begin{cases} R_k, & k = j \\ 0, & k \neq j \end{cases} \end{aligned} \tag{5}$$

where, Q is the continuous process noise covariance, R_k is the discrete measurement noise covariance, $\delta(\cdot)$ is the Dirac delta function, δ_{kj} is the Kronecker delta function and k is the discrete index. The random variables $\mathbf{w}$ and $\mathbf{v}_k$ are commonly denoted as $\mathbf{w} \sim \mathcal{N}(0, Q)$ and $\mathbf{v}_k \sim \mathcal{N}(0, R_k)$ respectively, where $\mathbf{w}$ and $\mathbf{v}_k$ are 0 mean distributions and of covariance Q and R_k respectively. The initial state of the system in Eq. (4) is assumed to be a Gaussian random vector with mean $\bar{\mathbf{x}}_0$ and covariance $\bar{P}_0$ and can be denoted as $\mathbf{x}_0 \sim \mathcal{N}(\bar{\mathbf{x}}_0, \bar{P}_0)$.

maps and simultaneously use these online maps generated to bound the errors that creep in due to errors in inertial navigation systems (INS).

[f]For the definition on observability of nonlinear systems, refer.[56]

Remark II.1 *For the approach proposed in this paper, the input* $\mathbf{u}(t)$ *can be assumed to be* 0 *which covers the case of an open-loop estimation problem or* $\mathbf{u}(t)$ *can be formed using the true value of the state vector which addresses the case of closed-loop estimation. In either case, the main issue that will be addressed is assessing the performance of the estimator.*

Remark II.2 *The Taylor series expansion for a vector valued function* $\mathbf{f}$ *of a vector argument* $\mathbf{x}$ *at the operating point* $\bar{\boldsymbol{\alpha}}$ *such that* $\mathbf{f}(\cdot) : \mathbf{x} \in \mathcal{R}^n \rightarrow \mathcal{R}^n$ *is given by*

$$\mathbf{f}(\mathbf{x}) = \mathbf{f}(\bar{\boldsymbol{\alpha}}) + \nabla \mathbf{f}(\mathbf{x})\Big|_{\mathbf{x}=\bar{\boldsymbol{\alpha}}} (\mathbf{x}-\bar{\boldsymbol{\alpha}}) + \frac{1}{2!}(\mathbf{x}-\bar{\boldsymbol{\alpha}})^T \nabla^2 \mathbf{f}(\mathbf{x})\Big|_{\mathbf{x}=\bar{\boldsymbol{\alpha}}} (\mathbf{x}-\bar{\boldsymbol{\alpha}}) + HOT \tag{6}$$

where, the operator $\nabla \mathbf{f}(\mathbf{x})$*, also called as the gradient, denotes the first partial differential of* $\mathbf{f}$ *with respect to* $\mathbf{x}$ *evaluated at the operating point* $\bar{\boldsymbol{\alpha}}$*,* $\nabla^2 \mathbf{f}(\mathbf{x})$ *denotes the Hessian of* $\mathbf{f}(\mathbf{x})$ *with respect to* $\mathbf{x}$ *and HOT denotes the higher order terms.*

Remark II.3 *Consider the nonlinear system*

$$\dot{\mathbf{x}}(t) = \mathbf{f}(\mathbf{x}(t)) \tag{7}$$

where $\mathbf{x} \in \mathcal{R}^n$ *is the state vector to be estimated and* $\mathbf{f}(\cdot) \in \mathcal{R}^n$ *represents the continuous time nonlinear dynamics that is a sufficiently smooth function. Then Eq. (7) can be discretized via an Euler series expansion of* $\mathbf{x}(t+\Delta t)$ *as*[41]

$$\mathbf{x}(t+\Delta t) = \mathbf{x}(t) + \dot{\mathbf{x}}(t)\Delta t + \ddot{\mathbf{x}}(t)(\Delta t)^2 + HOT \tag{8}$$

where, $\dot{\mathbf{x}}(t) \equiv \frac{d\mathbf{x}}{dt}$*,* $\ddot{\mathbf{x}}(t) \equiv \frac{d^2\mathbf{x}}{dt^2}$*,* Δt *denotes a small time step and HOT represent higher order terms. A first order Euler expansion follows as*

$$\begin{aligned} \mathbf{x}(t+\Delta t) &= \mathbf{x}(t) + \dot{\mathbf{x}}(t)\Delta t \\ \Rightarrow \dot{\mathbf{x}}(t) &= \frac{\mathbf{x}(t+\Delta t) - \mathbf{x}(t)}{\Delta t} \end{aligned} \tag{9}$$

A. Extended Kalman Filter

The goal of the extended Kalman filter (EKF) is to obtain an estimate of the systems state vector given by $\mathbf{x}(t)$ *in Eq. (4) by using the set of available measurements given by* $\mathbf{z}_k$ *in Eq. (4).*

1. EKF Filter Initialization

The EKF simulations start with the initialization of the EKF state estimates, $\hat{\mathbf{x}}(t)$ and the state error covariance matrix, $P(t)$ at $t = 0$. These are given in equations below as:

$$\begin{aligned} \hat{\mathbf{x}}(0) &= \hat{\mathbf{x}}_0 = E[\mathbf{x}(0 \cdot \Delta t)] = E[\mathbf{x}_0] \\ P(0) &= P_0 = E\left[(\mathbf{x}_0 - \hat{\mathbf{x}}_0)(\mathbf{x}_0 - \hat{\mathbf{x}}_0)^T\right] \end{aligned} \tag{10}$$

where, $\hat{\mathbf{x}}_0$ denotes the initial EKF state estimate, P_0 denotes the EKF initial state error covariance matrix, $\mathbf{x}_0$ denotes the model initial state and Δt is the sample time in seconds.

Remark II.4 *The design of the extended Kalman filter (EKF) is accomplished in two stages, which are*

1. *Prediction Stage, and*
2. *Update Stage.*

In the prediction stage, the filter predicts the estimate of the state vector via the nonlinear mapping in Eq. (4) based on the previous estimate of the state vector. In the update stage, the filter corrects the predicted estimate of the state obtained in the prediction stage with the available measurement at the current time instant.

Remark II.5 *Since the process model given by the first equation of Eq. (4) is in continuous time and the measurement equation in Eq. (4) is in discrete time, the continuous time state estimate prediction,* $\hat{\mathbf{x}}(t)$*, and the state error covariance matrix prediction,* $P(t)$*, at time t derived via Euler integration form the inputs to the update stage as* $\hat{\mathbf{x}}_k^-$ *and* P_k^- *respectively. Furthermore, after the update stage at discrete time k, the updated state estimate,* $\hat{\mathbf{x}}_k$*, and the updated state error covariance estimate,* P_k*, form the inputs to the prediction equations at* $t = t + \Delta t$*.*

2. EKF Prediction Equations

In the prediction stage of the EKF, the EKF state vector, at t is predicted via the nonlinear map given by $\mathbf{f}(\mathbf{x}(t), \mathbf{u}(t))$ based on the EKF estimate at $t - \Delta t$. Thus the prediction equations for an EKF are given below as

$$\begin{aligned} \dot{\hat{\mathbf{x}}}(t) &= \mathbf{f}(\hat{\mathbf{x}}(t), \mathbf{u}(t)) \\ \dot{P}(t) &= F(t) P(t) + P(t) F^T(t) + \Gamma Q \Gamma^T \\ F(t) &= \frac{\partial \mathbf{f}(\mathbf{x}(t), \mathbf{u}(t))}{\partial \mathbf{x}(t)}\Big|_{\mathbf{x}(t)=\hat{\mathbf{x}}(t), \mathbf{u}(t)} \end{aligned} \tag{11}$$

where, $\hat{\mathbf{x}}_k = \hat{\mathbf{x}}(k\Delta t)$ is the state estimate at k, $P_k = P(k\Delta t)$ is the state error covariance estimate at k, $F(t)$ is the partial derivative of the state nonlinear map with respect to the state vector evaluated at the EKF state estimate at t and Q is the continuous process noise covariance matrix given by Eq. (5).

3. EKF Transition to Update Stage

Since the problem formulation considered here is for a continuous process and discrete measurement, the prediction equations are in continuous time while the update equations need to be in discrete time. Therefore, after the prediction of the state estimate and the state error covariance estimate is performed at t, the correction to the state estimate and the state error covariance estimate is performed by sampling $\hat{\mathbf{x}}(t)$ and $P(t)$ as

$$\begin{aligned} \hat{\mathbf{x}}_k^- &= \hat{\mathbf{x}}(k\Delta t) + \dot{\hat{\mathbf{x}}}(t) \cdot \Delta t \\ P_k^- &= P(k\Delta t) + \dot{P}(t) \cdot \Delta t \end{aligned} \tag{12}$$

where, $\hat{\mathbf{x}}_k^-$ is the discrete predicted state estimate and P_k^- is the discrete predicted state error covariance at k.

4. EKF Update Equations

The final stage in the design of the EKF is the update stage. The update or correction to the EKF prediction is performed via the available measurements. The equations are given as

$$\begin{aligned} K_k &= P_k^- H_k^T \left(H_k P_k^- H_k^T + R_k\right)^{-1} \\ \hat{\mathbf{x}}_k &= \hat{\mathbf{x}}_k^- + K_k \left(\mathbf{z}_k - \hat{\mathbf{z}}_k^-\right), \quad \hat{\mathbf{z}}_k^- = \mathbf{h}\left(\hat{\mathbf{x}}_k^-\right) \\ P_k &= \left(I - K_k H_k\right) P_k^- \\ H_k &= \frac{\partial \mathbf{h}(\mathbf{x}_k)}{\partial \mathbf{x}_k}\Big|_{\mathbf{x}_k=\hat{\mathbf{x}}_k^-} \end{aligned} \tag{13}$$

where, $\hat{\mathbf{x}}_k$ is the corrected/update state estimate at k based on the available measurement at k given by $\mathbf{z}_k$, P_k is the corrected/updated state error covariance matrix at k, H_k is the linearized measurement matrix, R_k is the measurement noise covariance matrix given by Eq. (5) and K_k is the Kalman gain matrix which is obtained by minimizing the mean square state error.[6] This minimization can be viewed as minimizing the trace of the state error covariance matrix $P_k = E\left[\mathbf{e}_k \mathbf{e}_k^T\right]$, where $\mathbf{e}_k \equiv \mathbf{x}_k - \hat{\mathbf{x}}_k$.

B. Error State Kalman Filter (ErKF)

Consider the nonlinear state space process model in the continuous time domain given by the first equation of Eq. (4), where, as mentioned $\mathbf{x}$ is the state vector, $\mathbf{u}$ is the control input and $\mathbf{w}$ is the process noise vector which is modeled as a band-limited white Gaussian noise process with a specified covariance specified by Q as given in Eq. (5). For the purpose of the derivation of an error-state process model, we neglect the input and process noise and consider the following simplified nonlinear process model

$$\dot{\mathbf{x}}(t) = \mathbf{f}(\mathbf{x}(t)) \tag{14}$$

where, $\mathbf{f}(\mathbf{x}) = \begin{bmatrix} f_1 & f_2 & \dots & f_n \end{bmatrix}^T \in \mathcal{R}^n$. Applying a small perturbation $\delta\mathbf{x}(t)$ around $\mathbf{x}(t)$ yields

$$\dot{\mathbf{x}}(t) + \delta\dot{\mathbf{x}}(t) = \mathbf{f}(\mathbf{x}(t) + \delta\mathbf{x}(t)) \tag{15}$$

Applying Taylor series expansion to the right hand side (RHS) about $\mathbf{x}$, and neglecting the time notation t for notational convenience

$$\begin{aligned} \mathbf{f}(\mathbf{x}(t) + \delta\mathbf{x}(t)) &= \mathbf{f}(\mathbf{x}(t)) + \nabla\mathbf{f}(\mathbf{x}(t))(\mathbf{x}(t) + \delta\mathbf{x}(t) - \mathbf{x}(t)) + \boldsymbol{\mathcal{O}}(t, \mathbf{x}(t), \delta\mathbf{x}(t)) \\ &= \mathbf{f}(\mathbf{x}(t)) + \nabla\mathbf{f}(\mathbf{x}(t))\delta\mathbf{x}(t) + \boldsymbol{\mathcal{O}}(t, \mathbf{x}(t), \delta\mathbf{x}(t)) \end{aligned} \tag{16}$$

where $\boldsymbol{\mathcal{O}}$ stands for higher order terms and $\nabla\mathbf{f}(\mathbf{x}) = \begin{bmatrix} \left(\frac{\partial f_1}{\partial \mathbf{x}}\right)^T & \left(\frac{\partial f_2}{\partial \mathbf{x}}\right)^T & \dots & \left(\frac{\partial f_n}{\partial \mathbf{x}}\right)^T \end{bmatrix}^T$ denotes the gradient (first partial derivative) of $\mathbf{f}(\mathbf{x})$ with respect to $\mathbf{x}$. Assuming small perturbation, i.e., $\delta\mathbf{x}$ is small such that $\delta\mathbf{x}^2 \approx 0$, substituting Eq. (16) in Eq. (15) yields

$$\dot{\mathbf{x}}(t) + \delta\dot{\mathbf{x}}(t) = \mathbf{f}(\mathbf{x}(t)) + \nabla\mathbf{f}(\mathbf{x}(t))\delta\mathbf{x}(t) + \boldsymbol{\mathcal{O}}(t, \mathbf{x}(t), \delta\mathbf{x}(t)) \tag{17}$$

Furthermore, substituting Eq. (14) in Eq. (17) and neglecting the higher order terms yields the following linear time varying system with $\delta\mathbf{x}$ as the state vector as

$$\delta\dot{\mathbf{x}}(t) = F(t)\delta\mathbf{x}(t) \tag{18}$$

where, $F(t) \equiv \nabla\mathbf{f}(\mathbf{x}(t))$. Further notice that the matrix F is *independent of the error state vector* $\delta\boldsymbol{x}$, thereby resulting in a linear model for the error state propagation. Discretizing Eq. (18) results in

$$\frac{\delta\mathbf{x}(t + \Delta t) - \delta\mathbf{x}(t)}{\Delta t} = F(t)\delta\mathbf{x}(t) \tag{19}$$

where, $\delta\dot{\mathbf{x}}(t)$ is approximated via a first order Euler series expansion as shown in Eq. (9). Further simplifying Eq. (19) results in

$$\begin{aligned} \delta\mathbf{x}(t + \Delta t) &= \delta\mathbf{x}(t) + F(t)\delta\mathbf{x}(t)\Delta t \\ &= (I + F(t)\Delta t)\delta\mathbf{x}(t) \end{aligned} \tag{20}$$

Denoting $\delta\mathbf{x}(t + \Delta t) \equiv \delta\mathbf{x}_{k+1}$, $\delta\mathbf{x}(t) \equiv \delta\mathbf{x}_k$, $F(t) \equiv F_k$ and $(I + F_k\Delta t) \equiv \Phi_k$, Eq. (20) further reduces to

$$\delta\mathbf{x}_{k+1} = \Phi_k\mathbf{x}_k \tag{21}$$

where Φ_k is the state transition matrix and Δt is the discretization time interval.

ErKF Operational Equations

Recall that the *exact* continuous-time plant is given as

$$\dot{\mathbf{x}}(t) = \mathbf{f}(\mathbf{x}(t)) \tag{22}$$

where $\mathbf{x} \in \mathcal{R}^n$ is the state vector to be estimated and $\mathbf{f}(\cdot) \in \mathcal{R}^n$ represents the continuous time nonlinear dynamics that is at least once differentiable. Assuming that the initial condition for the state $\mathbf{x}(t)|_{t=0}$ is known, (22) can be integrated over a time interval $(0, \Delta t)$ to obtain

$$\mathbf{x}(t) = \int_0^{\Delta t} \mathbf{f}(\mathbf{x}(t))\, dt \tag{23}$$

Sampling the continuous time function $\mathbf{x}(t)$ at a period of Δt, yields the discretized version of Eq. (23), i.e., $\mathbf{x}(t)|_{t=k\Delta t}$ where $k = 0, 1, \dots, K$. In the error-state filter design presented in,[50,51] the predicted state is considered to be the discretized version of the result of the plant integration carried out in (23).

$$\hat{\mathbf{x}}_k^- = \mathbf{x}(t)|_{t=k\Delta t} \tag{24}$$

where, $\hat{\mathbf{x}}_k^-$ is the predicted estimate at k and $\mathbf{x}(t)|_{t=k\Delta t}$ is obtained from (23). Furthermore, consider the continuous time state space model that forms the basis of the Kalman filter. The (linearized) error-state process model obtained in Eq. (18), augmented by process noise is given by

$$\delta\dot{\mathbf{x}}(t) = F(t)\,\delta\mathbf{x}(t) + \Gamma\mathbf{w}(t) \tag{25}$$

where $\delta\mathbf{x}(t) \in \mathcal{R}^n$ is the error state (errors in state $\mathbf{x}(t)$), $F(\mathbf{x}(t)) \in \mathcal{R}^{n\times n}$ is the system matrix, $\mathbf{w} \in \mathcal{R}^{n_w}$ is the process noise vector and $\Gamma \in \mathcal{R}^{n\times n_w}$ is the process noise gain matrix. As can see from Eq. (25), ***the error-state process model is linear***. Similar to the discretization followed to obtain Eq. (18), the continuous time error state process model in Eq. (25) is discretized to obtain

$$\delta\mathbf{x}_k = \Phi_{k-1}\delta\mathbf{x}_{k-1} + \tilde{\mathbf{w}}_{k-1} \tag{26}$$

where $\tilde{\mathbf{w}}_{k-1} = \int_0^{\Delta t}\Phi(t,0)\,\Gamma\mathbf{w}(t)dt$ is the discretized process noise and Φ_{k-1} is the state transition matrix.[57] The measurement model is assumed to be in direct discrete time[57]

$$\mathbf{z}_k = \mathbf{h}(\mathbf{x}_k) + \mathbf{v}_k \tag{27}$$

where $\mathbf{z} \in \mathcal{R}^l$ is the $l-$dimensional measurement vector, $\mathbf{h}(\cdot)$ is the nonlinear measurement map as defined in Eq. (4) and $\mathbf{v} \sim \mathcal{N}(0, R_k)$ is the measurement noise assumed to be zero-mean white Gaussian (and uncorrelated with process noise $\mathbf{w}$) with a covariance denoted by R_k as shown in Eq. (5). The error-state predictions are modeled to be 0 as followed in.[50,51] This has the effect of resetting the predicted error at each time instant since in an ErKF implementation, the instantaneous error is of interest rather than the error history. In other words, the predicted error from the ErKF, denoted by $\delta\hat{\mathbf{x}}_k^-$, consists of small perturbations and is modeled as a zero mean process conditioned on all measurements obtained up to and including time instant $k-1$. Assuming that the initial state $\mathbf{x}_{0|0}$, the initial error state $\delta\mathbf{x}_{0|0}$ and the initial error state covariance $P_{0|0}$ are known, the error state covariance matrix is propagated using

$$P_k^- = \Phi_{k-1}P_{k-1}\Phi_{k-1}^T + Q_{k-1} \tag{28}$$

where Q_{k-1} is the discrete time equivalent process noise covariance matrix and is given by

$$Q_{k-1} = \int_0^{\Delta t}\Phi(t,0)\,\Gamma Q\Gamma^T\Phi^T(t,0)\;dt \tag{29}$$

where, $\Phi(t,0) = e^{F(t)t}$ is the continuous time state transition matrix and Q is the continuous time process covariance matrix given by Eq. (5). The innovation process, denoted by $\boldsymbol{\mathcal{I}}_k$, is

$$\boldsymbol{\mathcal{I}}_k = \mathbf{z}_k - \mathbf{h}\left(\hat{\mathbf{x}}_k^-\right) \tag{30}$$

where $\hat{\mathbf{x}}_k^-$ is obtained via Eqs. (23) and (24). It is worthwhile noticing that the predicted state obtained via integration and discretization of the exact plant from (3) is *fed-forward* into the ErKF. The innovation covariance, S_k, and the Kalman filter gain, K_k, can be computed as follows[6]

$$\begin{aligned} S_k &= R_k + H_kP_k^-H_k^T \\ K_k &= P_k^-H_k^TS_k^{-1} \end{aligned} \tag{31}$$

where H_k is the Jacobian as defined in Eq. (13), while the updated error state estimate and the updated state estimate are computed as

$$\begin{aligned} \delta\hat{\mathbf{x}}_k &= K_k\boldsymbol{\mathcal{I}}_k \\ \hat{\mathbf{x}}_k &= \hat{\mathbf{x}}_k^- + \delta\hat{\mathbf{x}}_k \end{aligned} \tag{32}$$

Finally, the updated error state covariance matrix is computed as

$$P_k = (I - K_kH_k)\,P_k^- \tag{33}$$

Notice that the updated error state estimate $\delta\hat{\mathbf{x}}_k$ does not contain the predicted error state estimate $\delta\hat{\mathbf{x}}_k^-$ as is the case with standard ErKF formulations.[50,51]

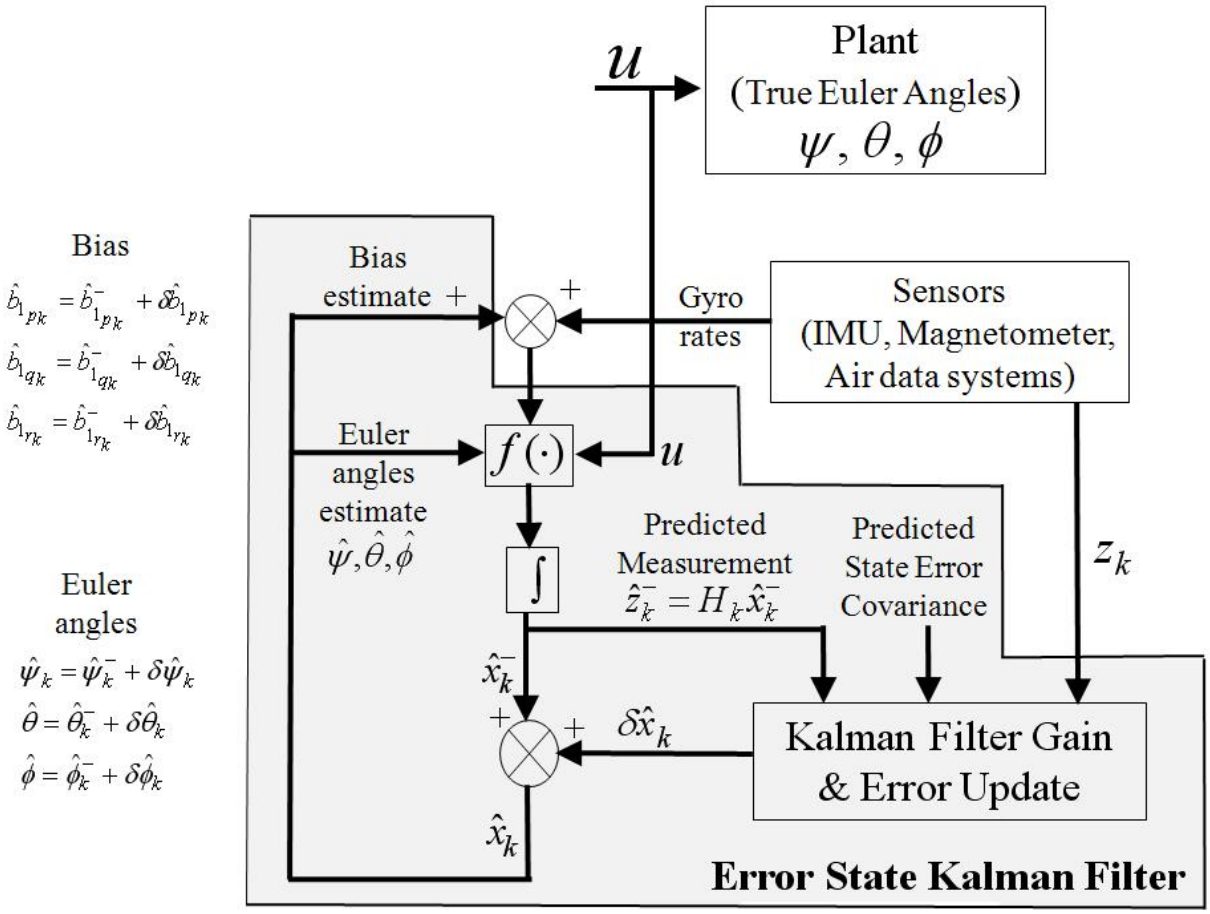

Figure 1. Block Diagram of a Typical ErKF Implementation.

C. Analytical difference between the EKF and the ErKF

The following remarks presented below attempt to uncover some of the underlying differences between the EKF and the ErKF.

Remark II.6 *The ErKF is used to only estimate the errors in the state vector, for e.g., estimating the errors in the Euler angles of an AHRS problem. In doing so, the ErKF recasts the nonlinear domain problem given by Eq. (22) to that of a time varying linear domain error estimation problem as given in Eq. (18), while the EKF attempts to estimate the states of the system represented by Eq. (22). The system matrix, $F(\mathbf{x})$, in an ErKF formulation is a function of the actual time varying plant states and not the error states and hence is considered to be time varying but otherwise linear. The system matrix, $F(\mathbf{x})$, in the EKF formulation is a function of the plant states which form the state vector of the EKF. Thus, this matrix is a linearized matrix, unlike in the ErKF case, which is a linear matrix.*

Remark II.7 *The state error covariance prediction for an ErKF follows from Eq. (28) where it can be seen that the state transition matrix is a discretized version of the linear time varying system matrix given by Eq. (18). The state error covariance prediction for the EKF, on the other hand, uses the fourth equation of Eq. (11) where the system matrix is a linearized version of the nonlinear plant about the current state trajectory. Hence the state error covariance prediction in the EKF is sub-optimal while the state error covariance prediction in the ErKF is optimal from the perspective of minimizing the root mean square error.*

Remark II.8 *The state error covariance prediction for an ErKF or an EKF is used as an input to computing the Kalman gain matrix as shown by Eq. (31) for an ErKF or by Eq. (13) for an EKF. Hence, any loss in optimality in the predicted state error covariance leads to loss in optimality in the computation of the Kalman gain matrix and further in the update of the state estimate based on the Kalman gain.*

III. Attitude Heading Reference System

We consider the problem of estimating the attitude[g] kinematics of a vehicle such as an aircraft which is performing a series of different maneuvers. A device to determine the aircraft's attitude is called as an attitude heading reference system[47,50,58–61] (AHRS). An AHRS consists of sensors on three axes that provide heading and attitude information for an aircraft. A typical AHRS for a small unmanned aircraft consist of either solid-state or Micro Electro Mechanical Systems (MEMS) gyroscopes, accelerometers[62–64] and magnetometers on all the three axes. The attitude information generated via an AHRS is used in many navigation guidance and control applications such as pilot-in-the-loop control of manned aircraft.[50] Furthermore, control devices such as autopilots use attitude information generated via an AHRS.

A. Truth Process

A 6 degree-of-freedom (DOF) model adapted from the open-source Flight Dynamics and Control toolbox (FDC)[h], is used for the simulation of the truth environment. The aircraft is trimmed at a Mach number of 0.3 and an altitude of 4000 meters. The following two scenarios were studied and analyzed:

1. 2 Doublets and a $3-2-1-1$ input are applied to the rudder. A doublet, shown in Figure 2(a), is an excitation function which consists of the following:

   i. a $+1$ amplitude step of a fixed duration, τ_{doub} (for e.g., 5 seconds), followed by

   ii. a -1 amplitude step input of the same duration.

   A $3-2-1-1$ input, shown in Figure 2(b), is an excitation function which consists of the following:

   i. a 3 second $+1$ amplitude step input, followed by

   ii. a 2 second -1 amplitude step input, followed by

   iii. a 1 second $+1$ amplitude step input, followed by

   iv. a 1 second -1 amplitude step input.

   These inputs excite the mildly unstable spiral mode[i]. A bank limiter is used to prevent the aircraft from spiraling out of control and limit the bank angle to 15 degrees. This input was chosen to study the tracking ability of the filters to aggressive inputs.

2. A coordinated banked turn[j] is performed at the same flight condition. The aircraft altitude is maintained fairly constant during the entire phase of the maneuver.

Both the scenarios described above are also run with the continuous Dryden[k] wind turbulence model, from the SIMULINK Aerospace blockset to study the performance of the filters in the presence of unmodeled dynamics. The Dryden Wind Turbulence Model (Continuous) block uses the Dryden spectral representation to add turbulence to the aerospace model by passing band-limited white noise through appropriate forming filters. This block implements the mathematical representation in the Military Specification $MIL-F-8785C$ and Military Handbook $MIL-HDBK-1797$.[66,67]

The truth model generated as described above yields truth parameters such as the Euler angles, $(\psi,\ \theta,\ \phi)$, angular rates, $(p,\ q,\ r)$ and accelerometer readings, $(a_x,\ a_y,\ a_z)$. We denote the quantities such as Euler angles as $(\psi_{model},\ \theta_{model},\ \phi_{model})$ and quantities such as angular rates and the accelerometer readings as $(p_m,\ q_m,\ r_m)$ and $(a_{x_m},\ a_{y_m},\ a_{z_m})$ to indicate that these form the gyroscope and accelerometer measurements respectively. The filter performance will be evaluated on the basis of being able to accurately reconstruct parameters such as $\psi_{model},\ \theta_{model},\ \phi_{model}$.

[g] By attitude we mean the vehicle's orientation in space.

[h] For details about FDC refer.[65]

[i] An aircraft's unstable spiral mode is a lateral mode characterized by high yaw rate and low turn radius.

[j] A coordinated banked turn is when an aircraft moves in a plane at a constant speed (magnitude of velocity vector) and turns with a constant angular rate.[57]

[k] For details about the Dryden wind turbulence model, refer.[66]

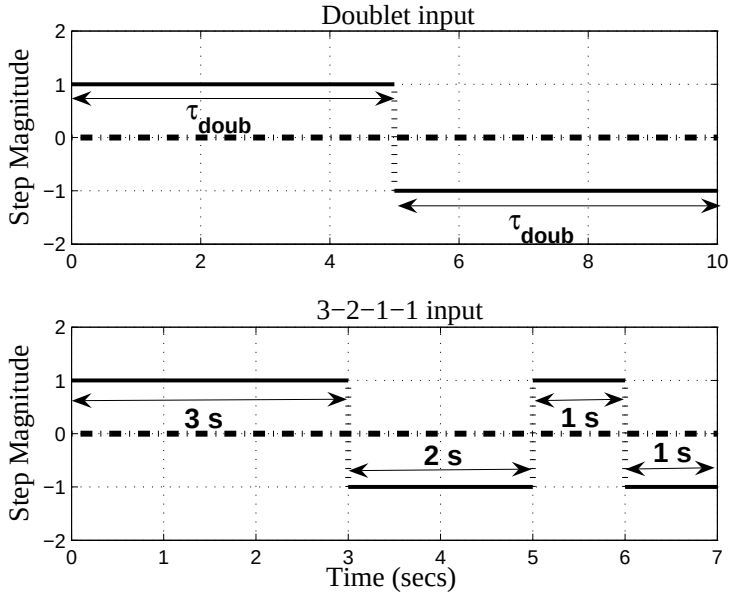

Figure 2. Functions that excite the natural frequencies of the aircraft.

B. Model for Filter Design

We consider the system of differential equations which describe the aircraft's attitude[l] in space parameterized via Euler angles as follows:[68,69]

$$\begin{aligned}
\dot{\psi}(t) &= q_m(t)\left(\frac{\sin\phi(t)}{\cos\theta(t)}\right) + r_m(t)\left(\frac{\cos\phi(t)}{\cos\theta(t)}\right) \\
\dot{\theta}(t) &= q_m(t)\cos\phi(t) - r_m(t)\sin\phi(t) \\
\dot{\phi}(t) &= p_m(t) + q_m(t)\left(\sin\phi(t)\tan\theta(t)\right) + r_m(t)\left(\cos\phi(t)\tan\theta(t)\right)
\end{aligned} \tag{34}$$

where, $\phi(t)$, $\theta(t)$, $\psi(t)$ are the Euler angles, in *radians*, that describe the aircraft attitude and are called as yaw, pitch & roll respectively, $\dot{\psi}(t)$, $\dot{\theta}(t)$ $\dot{\phi}(t)$ are the Euler angle rates in *radians/sec* and $p_m(t)$, $q_m(t)$, $r_m(t)$ are the components of the angular velocity, in *radians/sec*, in the body frame[m]. More precisely, $p_m(t)$, $q_m(t)$, $r_m(t)$ are the angular rate measurements obtained from a triad of orthogonal rate gyroscopes, where $p_m(t)$ is the output of the rate gyroscope with its sensing axis aligned with the roll axis, $q_m(t)$ is the output of the pitch axis rate gyroscope and $r_m(t)$ is the output of the yaw axis rate gyroscope.[50]

1. Gyroscope Model

In a general problem formulation, the measurements $p_m(t)$, $q_m(t)$, $r_m(t)$ are composed of the actual values and noise and are assumed to be in the following mathematical form:[50,70]

$$\begin{aligned}
p_m(t) &= p + \underbrace{b_{1_p} + b_{t_p}(t) + b_{w_p}(t)}_{b_p(t)\ =\ bias\ in\ p} \\
q_m(t) &= q + \underbrace{b_{1_q} + b_{t_q}(t) + b_{w_q}(t)}_{b_q(t)\ =\ bias\ in\ q} \\
r_m(t) &= r + \underbrace{b_{1_r} + b_{t_r}(t) + b_{w_r}(t)}_{b_r(t)\ =\ bias\ in\ r}
\end{aligned} \tag{35}$$

[l]For the full set of aircraft equations of motion in the body frame, refer.[68,69]

[m]By body frame, we mean a rotating, non-inertial frame that moves with the aircraft, i.e. fixed to the aircraft and an inertial frame is one wherein the origin may be any point that is completely unaccelerated.

where, $p,\ q,\ r$ are the **true** components of the angular velocity (yaw, pitch, roll) in *radians/sec*, $b_{1_p},\ b_{1_q},\ b_{1_r}$ are called as the *constant null-shift* bias terms, $b_{t_p}(t),\ b_{t_q}(t),\ b_{t_r}(t)$ are called as the *time varying* bias components in $p,\ q,\ r$ and $b_{w_p}(t),\ b_{w_q}(t),\ b_{w_r}(t)$ denote the error due to *sampling noise* which is typically wideband noise.[50] These bias components denote the errors in the true values of $p,\ q,\ r$ whenever these measuring devices are switched on.

Remark III.1 *For the purpose of this paper, we consider the effects of constant bias and bias due to wide-band noise. The effect due to constant bias, however, is modeled in the filter as a Weiner process*[n] *which is achieved by integrating band-limited white noise of zero mean and a specified covariance.*[70] *One could think of modeling the constant bias term in the filter as zero derivative states; however by doing so the corresponding entries in the Q matrix are set to* 0 *which could then lead to the phenomenon of divergence. Thus, we model the constant bias states in the filter as a Weiner process thereby ensuring that there is some robustness in the process model.*

Based on Remark III.1, the bias models for the filter design are as follows:

$$\begin{aligned} \dot{b}_{1_p}(t) &= w_{b_{1_p}} \\ \dot{b}_{1_q}(t) &= w_{b_{1_q}} \\ \dot{b}_{1_r}(t) &= w_{b_{1_r}} \end{aligned} \tag{36}$$

where, $w_{b_{1_p}},\ w_{b_{1_q}},\ w_{b_{1_r}}$ represent the process driving noise which are zero mean, band-limited white noise with specified standard deviations as $\sigma_{b_{1_p}},\ \sigma_{b_{1_q}},\ \sigma_{b_{1_r}}$. Furthermore, the components of the error source corresponding to sampling noise, $b_{w_p}(t),\ b_{w_q}(t),\ b_{w_r}(t)$, are typically modeled as band-limited white noise of zero mean and a specified covariance as:

$$\begin{aligned} b_{w_p}(t) &= w_{b_{w_p}} \\ b_{w_q}(t) &= w_{b_{w_q}} \\ b_{w_r}(t) &= w_{b_{w_r}} \end{aligned} \tag{37}$$

where, $w_{b_{w_p}},\ w_{b_{w_q}},\ w_{b_{w_r}}$ denote the band-limited, zero mean, white Gaussian noise processes of covariances $\sigma^2_{b_{w_p}},\ \sigma^2_{b_{w_q}}$ and $\sigma^2_{b_{w_r}}$ respectively.

2. Accelerometer Model

In addition to the gyroscope measurements that provide the rate outputs $p_m(t),\ q_m(t),\ r_m(t)$, there are 3 accelerometers that provides the proper acceleration (acceleration relative to free-fall), in terms of g-force. These accelerometer measurement readings are denoted as $a_{x_m},\ a_{y_m},\ a_{z_m}$ and are given by an additive combination of the true accelerometer readings and noise. Thus, mathematically, the accelerometer measurements are formulated as

$$\begin{aligned} a_{x_m}(t) &= a_x + w_{a_x}(t) \\ a_{y_m}(t) &= a_y + w_{a_y}(t) \\ a_{z_m}(t) &= a_z + w_{a_z}(t) \end{aligned} \tag{38}$$

where, $a_x,\ a_y,\ a_z$ are the **true** components of the accelerometer measurements and $w_{a_x},\ w_{a_y},\ w_{a_z}$ denote the noise processes respectively for the $x,\ y,\ z$ axes accelerometers which are modeled as zero mean band-limited Gaussian white noise processes with specified covariances given by $\sigma^2_{a_x},\ \sigma^2_{a_y},\ \sigma^2_{a_z}$, where $\sigma_{a_x},\ \sigma_{a_y},\ \sigma_{a_z}$ denote the standard deviations of the respective noise processes associated with the accelerometer measurements.

Remark III.2 *The gyroscope measurements ($p_m,\ q_m,\ r_m$), accelerometer measurements ($a_{x_m},\ a_{y_m},\ a_{z_m}$), magnetometer measurement (ϕ_{meas}) and the true air speed measurement (V_{TAS}) form the original measurement set, while the Euler angles $\theta_{meas},\ \phi_{meas}$ form the derived measurement set.*

[n] Weiner process is also known as a random walk process.

3. Filter Model: Process and Measurement

Using Remark III.1, neglecting the time varying bias terms, $b_{t_p},\ b_{t_q},\ b_{t_r}$, in Eq. (35), substituting Eq. (35) into Eq. (34), dropping the argument t and further simplifying, results in

$$\begin{aligned}
\dot{\psi} &= q\left(\frac{\sin\phi}{\cos\theta}\right) + r\left(\frac{\cos\phi}{\cos\theta}\right) + b_{w_q}\left(\frac{\sin\phi}{\cos\theta}\right) + b_{1_q}\left(\frac{\sin\phi}{\cos\theta}\right) + b_{w_r}\left(\frac{\cos\phi}{\cos\theta}\right) + b_{1_r}\left(\frac{\cos\phi}{\cos\theta}\right) \\
\dot{\theta} &= q\cos\phi - r\sin\phi + b_{w_q}\cos\phi + b_{1_q}\cos\phi - b_{w_r}\sin\phi - b_{1_r}\sin\phi \\
\dot{\phi} &= p + q\left(\sin\phi\tan\theta\right) + r\left(\cos\phi\tan\theta\right) + b_{w_p} + b_{1_p} + b_{w_q}\left(\sin\phi\tan\theta\right) + b_{1_q}\left(\sin\phi\tan\theta\right) \\
&\quad + b_{w_r}\left(\cos\phi\tan\theta\right) + b_{1_r}\left(\cos\phi\tan\theta\right)
\end{aligned} \tag{39}$$

Furthermore, with the following notations $\sin\phi \equiv s\phi$, $\sin\theta \equiv s\theta$, $\cos\phi \equiv c\phi$, $\cos\theta \equiv c\theta$ and $\tan\theta \equiv t\theta$, and augmenting the bias states given in Eq. (36) to Eq. (39) the process equations can be re-written as

$$\begin{aligned}
\dot{\psi} &= \underbrace{q\left(\frac{s\phi}{c\theta}\right) + r\left(\frac{c\phi}{c\theta}\right) + b_{1_q}\left(\frac{s\phi}{c\theta}\right) + b_{1_r}\left(\frac{c\phi}{c\theta}\right)}_{f_1} + b_{w_q}\left(\frac{s\phi}{c\theta}\right) + b_{w_r}\left(\frac{c\phi}{c\theta}\right) \\
\dot{\theta} &= \underbrace{qc\phi - rs\phi + b_{1_q}c\phi - b_{1_r}s\phi}_{f_2} + b_{w_q}c\phi - b_{w_r}s\phi \\
\dot{\phi} &= \underbrace{p + q\ s\phi\ t\theta + r\ c\phi\ t\theta + b_{1_p} + b_{1_q}s\phi\ t\theta + b_{1_r}c\phi\ t\theta}_{f_3} + b_{w_p} + b_{w_q}s\phi\ t\theta + b_{w_r}c\phi\ t\theta \\
\dot{b}_{1_p} &= w_{b_{1_p}} \\
\dot{b}_{1_q} &= w_{b_{1_q}} \\
\dot{b}_{1_r} &= w_{b_{1_r}}
\end{aligned} \tag{40}$$

Furthermore, the **force equations** for a 6 DOF aircraft are given by

$$\begin{aligned}
X &= m\left(\dot{u}^E + qw^E - rv^E\right) + mgs\theta \\
Y &= m\left(\dot{v}^E + ru^E - pw^E\right) - mgc\theta s\phi \\
Z &= m\left(\dot{w}^E + pv^E - qu^E\right) - mgc\theta c\phi
\end{aligned} \tag{41}$$

where, $X,\ Y,\ Z$ are the components of the resultant aerodynamic force acting on the aircraft in body axis frame, $\left(u^E,\ v^E,\ w^E\right)$ are the GPS components of the aircraft ground speed expressed in the body frame, m is the mass of the aircraft and g is the acceleration due to gravity. The terms $\frac{X}{m},\ \frac{Y}{m},\ \frac{Z}{m}$ are the accelerometer readings in the body $(x,\ y,\ z)$ axes and are given by $a^*_{x_m}, a^*_{y_m}, a^*_{z_m}$, respectively.[o] Using the accelerometer measurement equations in Eq. (38) and Remark III.1, the roll and pitch measurement model for the design of the filter becomes:

$$\begin{aligned}
\theta_{meas} &= \sin^{-1}\left(\frac{a^*_{x_m} - \dot{u}^E + r^*_m v^E - q^*_m w^E}{g}\right) \\
\phi_{meas} &= \tan^{-1}\left(\frac{a^*_{y_m} - \dot{v}^E + p^*_m w^E - r^*_m u^E}{a^*_{z_m} - \dot{w}^E + q^*_m u^E - p^*_m v^E}\right)
\end{aligned} \tag{42}$$

where $\theta_{meas},\ \phi_{meas}$ are measurements derived from the accelerometer and gyroscope readings, $(p^*_m,\ q^*_m,\ r^*_m)$ are the obtained gyroscope measurements[p] and $\left(\dot{u}^E,\ \dot{v}^E,\ \dot{w}^E\right)$ are the inertial linear accelerations of the aircraft center of gravity (CG) expressed in the body frame. Note that the second equation of Eq. (42) (ϕ_{meas}) is obtained by dividing the second equation of Eq. (41) by the third equation of Eq. (41) and then using the inverse tangent function.

Assumption III.3 *For a more realistic problem formulation the following assumptions are made:*[73]

[o]The modeled accelerometer measurements given in Eq. (38) need not necessarily be the same as the obtained accelerometer measurements.

[p]The modeled gyro measurements given in Eq. (35) need not necessarily be the same as the obtained gyro measurements.

1. *Since it is not possible to estimate the aircraft accelerations in the body frame, the following terms are set to 0: $\dot{u}^E = 0,\ \dot{v}^E = 0,\ \dot{w}^E = 0$, i.e., the aircraft CG is assumed completely unaccelerated with respect to the inertial frame. This assumption is, however, not valid if the aircraft maneuvers rapidly.*

2. *$u^E = V_{TAS},\ v^E = 0,\ w^E = V_d$, where V_{TAS} is the aircraft true airspeed and V_d is the aircraft downward speed.*

It is assumed that the quantity V_{TAS} is obtained via a pressure sensor.

Using Assumption III.3 in the first and second equations of Eq. (42), the measurement model simplifies to

$$\begin{aligned} \theta_{meas} &= \sin^{-1}\left(\frac{a^*_{x_m} - q^*_m V_d}{g}\right) \\ \phi_{meas} &= \tan^{-1}\left(\frac{a^*_{y_m} + p^*_m V_d - r^*_m V_{TAS}}{a^*_{z_m} + q^*_m V_{TAS}}\right) \end{aligned} \tag{43}$$

Furthermore, a magnetometer[q] is used to generate the aircraft heading measurement of the aircraft. This measurement, denoted as ψ_{meas}, is obtained by adding zero mean Gaussian band-limited white noise of a specified covariance, σ^2_ψ, to ψ_{model}, which is generated from the truth model, as

$$\psi_{meas} = \psi_{model} + w_\psi \tag{44}$$

where, w_ψ is zero mean Gaussian band-limited white noise, typically denoted as $w_\psi \sim \mathcal{N}\left(0, \sigma^2_\psi\right)$. Thus the final measurement model for the design of the EKF or the ErKF is the combination of Eqs. (43) and (44). It is assumed that the input $\mathbf{u}(t) = 0$, thereby treating a purely estimation problem in this paper. Comparing the model in Eq. (40) with Eq. (4), it can be seen that

$$\begin{aligned} \mathbf{x}(t) &= \begin{bmatrix} \psi & \theta & \phi & b_{1_p} & b_{1_q} & b_{1_r} \end{bmatrix}^T, \quad \mathbf{f}(\mathbf{x}(t)) = \begin{bmatrix} f_1 & f_2 & f_3 & 0 & 0 & 0 \end{bmatrix}^T \\ \mathbf{w}(t) &= \begin{bmatrix} b_{w_p} \\ b_{w_q} \\ b_{w_r} \\ w_{b_{1_p}} \\ w_{b_{1_q}} \\ w_{b_{1_r}} \end{bmatrix}, \quad \Gamma = \begin{bmatrix} 0 & \frac{s\phi}{c\theta} & \frac{c\phi}{c\theta} & 0 & 0 & 0 \\ 0 & c\phi & -s\phi & 0 & 0 & 0 \\ 1 & s\phi\ t\theta & c\phi\ t\theta & 0 & 0 & 0 \\ 0 & 0 & 0 & 1 & 0 & 0 \\ 0 & 0 & 0 & 0 & 1 & 0 \\ 0 & 0 & 0 & 0 & 0 & 1 \end{bmatrix}, \quad H_k = \begin{bmatrix} 1 & 0 & 0 & 0 & 0 & 0 \\ 0 & 1 & 0 & 0 & 0 & 0 \\ 0 & 0 & 1 & 0 & 0 & 0 \end{bmatrix} \end{aligned} \tag{45}$$

where, given that the measurements are the Euler angles $\psi,\ \theta,\ \phi$, the measurement function $\mathbf{h}(\mathbf{x}_k)$ in Eq. (4) reduces to a linear matrix of the form $H_k\mathbf{x}_k$, where H_k is as shown in Eq. (45). The noise covariance matrices are found to be

$$Q = \begin{bmatrix} \sigma^2_{b_{1_p}} & 0 & 0 & 0 & 0 & 0 \\ 0 & \sigma^2_{b_{1_q}} & 0 & 0 & 0 & 0 \\ 0 & 0 & \sigma^2_{b_{1_r}} & 0 & 0 & 0 \\ 0 & 0 & 0 & \sigma^2_{b_{w_p}} & 0 & 0 \\ 0 & 0 & 0 & 0 & \sigma^2_{b_{w_q}} & 0 \\ 0 & 0 & 0 & 0 & 0 & \sigma^2_{b_{w_r}} \end{bmatrix}, \ R_k = \begin{bmatrix} \sigma^2_\psi & 0 & 0 \\ 0 & \sigma^2_\theta & 0 \\ 0 & 0 & \sigma^2_\phi \end{bmatrix} \tag{46}$$

where, σ^2_θ and σ^2_ϕ are the covariances of θ_{meas} and ϕ_{meas} respectively. The standard deviation values are chosen as follows: $\sigma_{b_{1_p}} = \sigma_{b_{1_q}} = \sigma_{b_{1_r}} = 0.05^\circ/s$ and $\sigma_\psi = \sigma_\theta = \sigma_\phi = 0.25^\circ$.[50] The standard deviation values for the bias wideband noise are chosen as follows: $\sigma_{b_{w_p}} = \sigma_{b_{w_q}} = \sigma_{b_{w_r}} = 0.001^\circ/s$. The initial state estimates of the EKF and the ErKF are set to 0, while an initial standard deviation of 5° is provided for the state estimates of the EKF and an initial standard deviation of 0.5° the ErKF.

[q] A magnetometer is a scientific instrument used to measure the strength and direction of the magnetic field in the vicinity of the instrument. The magnetometer provides the magnetic heading which needs to be added to the magnetic variation to yield the vehicle heading with respect to the true north.

IV. Simulation Results

In this section, we present some results which compare the performances of the EKF and the ErKF with respect to estimating the attitude kinematics $(\psi,\ \theta,\ \phi)$ of an aircraft along with gyroscope bias via an attitude heading reference system model. We consider the case where the bias in the gyroscope model is accounted for in the model of the EKF and the ErKF and a second case where the bias in the gyroscope model is NOT accounted for either in the EKF or in the ErKF. The importance of accounting for a good bias model is illustrated in the second case. In the discussion presented below, we start by looking at the various maneuvers that are performed by an aircraft for which the performances of the EKF and the ErKF are compared.

Remark IV.1 *The intent of the simulations is to show that the ErKF, once initially tuned, is robust to a suite of aircraft maneuvers, unlike the EKF which would otherwise require re-tuning for different maneuvers or flight atmospheric conditions such as the presence or absence of wind turbulence. Naturally, the EKF could, conceivably, be tuned to its best capability for each of these maneuvers and exhibit acceptable estimation performance. However, the goal of this paper is to evaluate the EKF and the ErKF in terms of their design parameter tuning robustness such that once the covariances are tuned for a particular maneuver, further re-tuning should not be required, irrespective of the type of maneuver that the aircraft performs.*

A. Simulated Aircraft Maneuvers

The following are the aircraft maneuvers for which estimation performance of the EKF and the ErKF are evaluated against each other. These maneuvers include:

1. Steady Level Flight with no limit on aircraft bank angle, as shown in Figure 3(a).
2. Steady Level Flight with a limit on aircraft bank angle of 15°, as shown in Figure 3(b).
3. Coordinated Turn at approximately constant altitude, as shown in Figure 3(c).

The true initial attitude of the aircraft is set to $\psi(0) = 0°$, $\theta(0) = 3.63°$ and $\phi(0) = 0°$, while the true initial position of the aircraft is $x(0) = 0\ m$, $y(0) = 0\ m$ and $z(0) = 4000\ m$. The true initial velocity components in the body frame are set to $u(0) = 100\ m/s$, $v(0) = 0\ m/s$ and $w(0) = 6\ m/s$. The aircraft starts at an initial latitude and longitude of 0° each. In each of the aircraft maneuvers shown in Figure 3, the starting position of the aircraft is represented by a 'o' and the final position is represented by a $'\times'$.

B. Modeled Gyroscope Bias

We consider the case where gyroscope bias presents itself in the measurements $(p_m,\ q_m,\ r_m)$ as *constant null-shift* bias and bias due to *sampling noise* effects which are represented as $(b_{1_p},\ b_{1_q},\ b_{1_r})$ and $(b_{w_p},\ b_{w_q},\ b_{w_r})$ respectively. Recall that $b_{1_p},\ b_{1_q},\ b_{1_r}$ are modeled as Wiener processes as shown by Eq. (36), while $b_{w_p},\ b_{w_q},\ b_{w_r}$ are modeled as band-limited white noise processes with specified covariances as shown by Eq. (37). The gyroscope bias in $b_{1_p},\ b_{1_q},\ b_{1_r}$ is uniformly set to $0.1°/s$.

Figures 4, 5 and 6 show the performances of an EKF and an ErKF respectively for the maneuvers shown in Figure 3. It can be seen from these figures that the estimation performance of the ErKF is superior to that of the EKF in estimating the Euler angles $\psi(t)$, $\theta(t)$, $\phi(t)$ and the gyroscope biases $b_{1_p},\ b_{1_q},\ b_{1_r}$. Specifically, Figures 4 and 5 clearly show the improvement in the estimation performance of the ErKF over the EKF. Furthermore, it should be pointed out here that though the performance of the EKF in estimating the roll angle for the maneuver depicted by Figure 3(c) is marginally better than that of the ErKF, as shown in Figure 6, this difference is still less than 0.5°. In addition, it can be seen from Figure 6 that the performance of the ErKF in estimating the yaw and pitch angles is much better than that of the EKF.

C. Unmodeled Gyroscope Bias

We further study the effect that unmodeled bias has on the performance of the EKF and the ErKF. To simulate this scenario we considered the aircraft maneuver depicted by Figure 3(a). The goal for this aspect of the study was to introduce bias in the gyroscope measurements via $b_{1_p},\ b_{1_q},\ b_{1_r}$ but **NOT** account for this in the model for the filter design. This implies that we perform estimation for the filter model given by

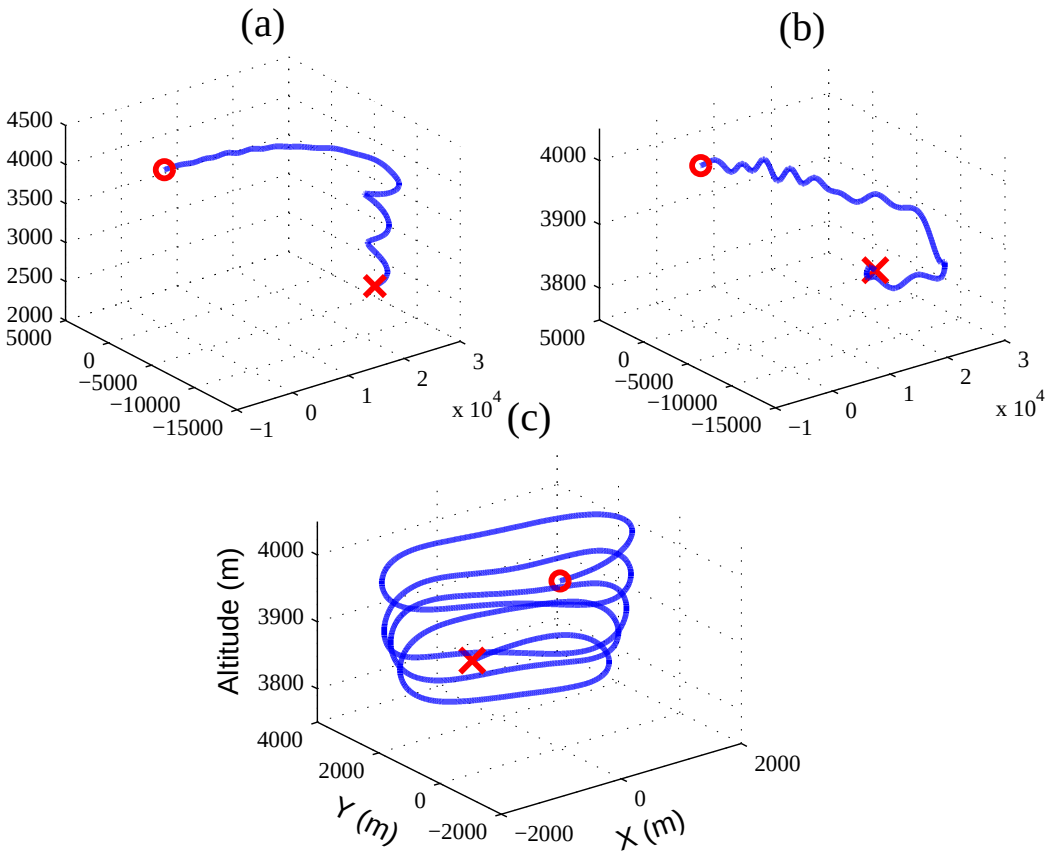

Figure 3. Different aircraft maneuvers for which attitude estimation is performed: (a) Steady Level Flight with no limit on aircraft bank angle, (b) Steady Level Flight with bank angle of 15° and (c) Coordinated Turn at approximately constant altitude.

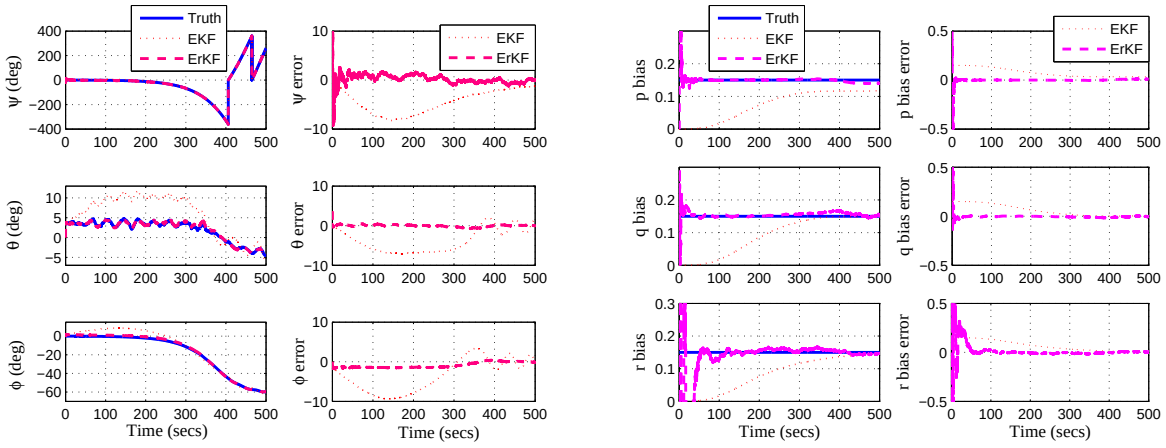

(a) Euler Angles

(b) Gyroscope Bias

Figure 4. Estimating the Euler angles and gyroscope bias for steady level flight with no limit on aircraft bank angle (Scenario depicted in figure 3(a)).

the equations in Eq. (34) with biased gyroscope measurements. The emphasis in this part of the study is to illustrate the effect that unmodeled bias has on the performance of either the EKF or the ErKF. Figure

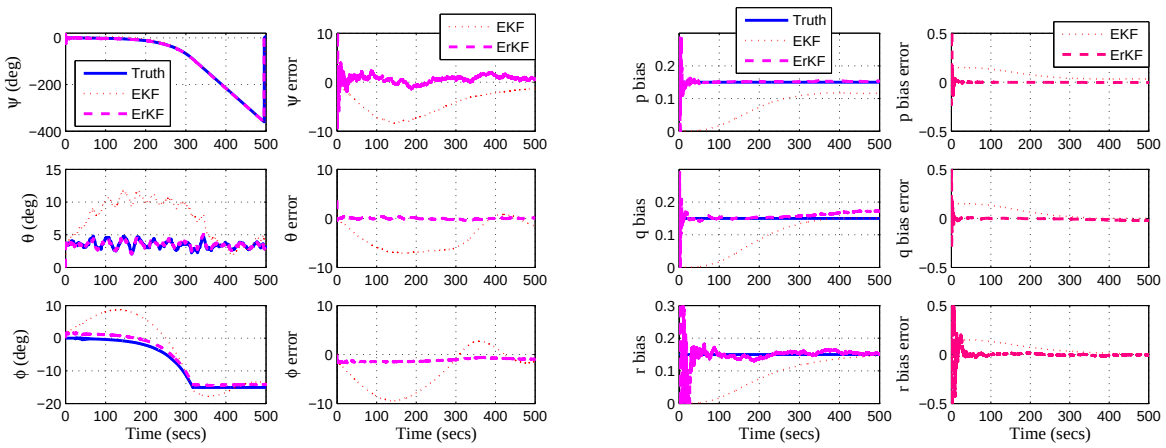

(a) Euler Angles (b) Gyroscope Bias

Figure 5. Estimating the Euler angles and gyroscope bias for steady level flight with a limit on aircraft bank angle of 15° (Scenario depicted in figure 3(b)).

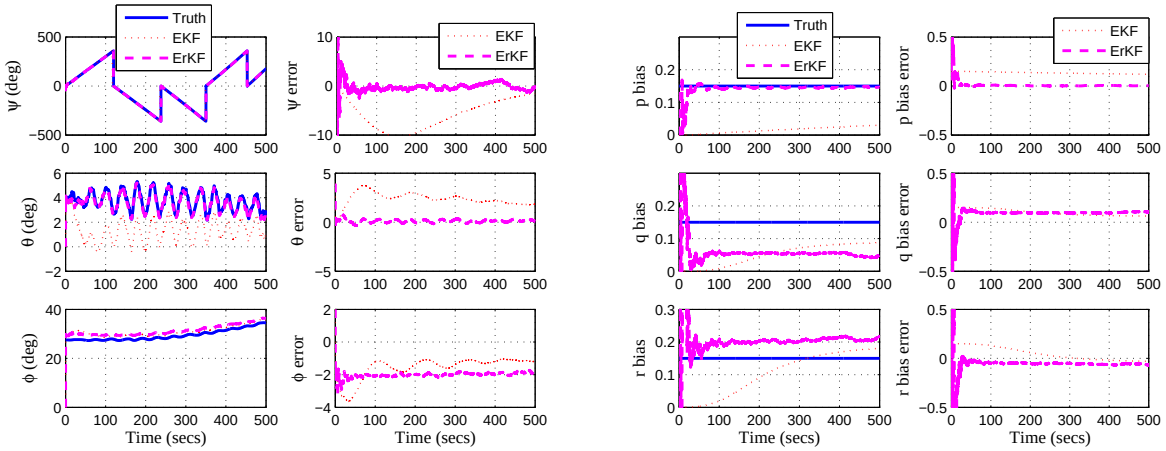

(a) Euler Angles (b) Gyroscope Bias

Figure 6. Estimating the Euler angles and gyroscope bias for a coordinated turn at approximately constant altitude (Scenario depicted in figure 3(c)).

7 shows the performance comparison between the EKF and ErKF, where the 3 sub-figures on the left hand side of the plot denote the estimation histories of the Euler angles and the 3 sub-figures on the right hand side of the plot depict the respective Euler angle estimation history errors. It can be seen that while the performance of both the filters is degraded due to the presence of unmodeled bias, the performance of the ErKF is still better than that of the EKF as can be seen by the estimation error plots.

V. Conclusion

The Kalman filter is the optimal minimum mean square estimator when the state and measurement dynamics are linear in nature, provided the process and measurement noise processes are modeled as white Gaussian. However, when the process model or the state propagation model is nonlinear, a class of algorithms called extended Kalman filters (EKF) have been traditionally used. EKFs work on the principle of linearizing the nonlinear dynamics, in order to apply the Kalman filter for state error covariance prediction and state estimate update. However, the EKFs while having been proven to work well for several applications, suffer from the curse of linearization errors. An alternative class of KF-based approaches called the error state KF

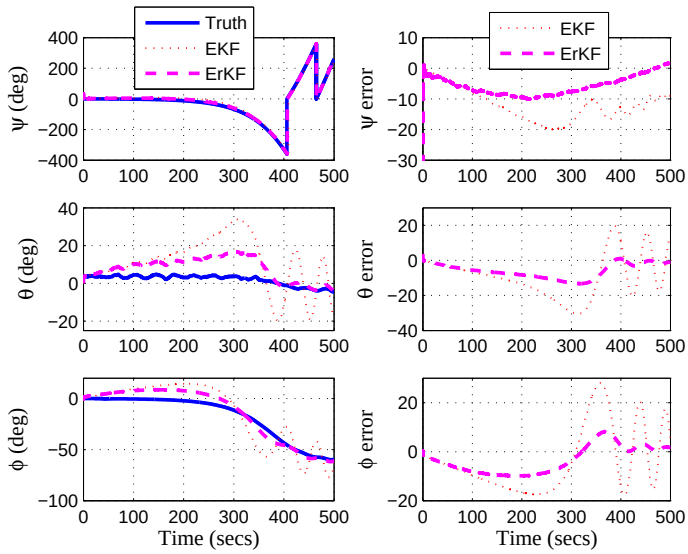

Figure 7. Estimating the Euler angles for scenario depicted in figure 3(a).

or the ErKF have been proposed and used, especially in robotics and air vehicle attitude estimation, that approaches the adaptation of nonlinear dynamics to the KF in a different manner to the EKF. The ErKF estimates the *error* in the state instead, as it turns out that under some fairly reasonable assumptions, the error propagation dynamics can be shown to be linear. Hence, when the error state instead of the full state itself, is estimated using the KF it lends itself to optimal updates and predictions as the (error) process model is linear. The present paper compares the EKF and ErKF filter-based approaches for the attitude estimation of an air vehicle, for three different simulated classes of maneuvers. It was observed from our simulations that the ErKF consistently obtained generally better, and in some cases significantly better, attitude estimates than the EKF, for a set of realistic process and measurement noise covariance tuning parameters. Furthermore, it was observed that to get the best results, i.e., with low errors, out of the EKF, it requires separate tuning for each class of maneuvers, while the ErKF performs satisfactorily with the same tuning for every maneuver. An additional advantage of the ErKF in attitude estimation problems during critical missions is that it is more robust to filter failures, i.e., even if the filter fails the attitudes can still be obtained via dead-reckoning (without compensation of errors), while this is not possible in the EKF as it contains the attitude angles itself in the state vector.

Appendix

Jacobian for EKF Prediction

The Jacobian matrix, $F(t)$, for the EKF prediction given by the fifth equation of Eq. (11) is obtained by computing the partial derivative of the nonlinear dynamics, $\mathbf{f}(\mathbf{x}(t))$, with respect to the state vector $\mathbf{x}(t)$, assuming that the input $\mathbf{u}(t) = 0$. With the definitions of $\mathbf{f}(\mathbf{x}(t))$ and $\mathbf{x}(t)$ given by Eq. (45), and ignoring the argument t from further analysis, the Jacobian results in

$$\frac{\partial \mathbf{f}(\mathbf{x})}{\partial \mathbf{x}} = \begin{bmatrix} \frac{\partial f_1}{\partial \psi} & \frac{\partial f_1}{\partial \theta} & \frac{\partial f_1}{\partial \phi} & \frac{\partial f_1}{\partial b_{1_p}} & \frac{\partial f_1}{\partial b_{1_q}} & \frac{\partial f_1}{\partial b_{1_r}} \\ \frac{\partial f_2}{\partial \psi} & \frac{\partial f_2}{\partial \theta} & \frac{\partial f_2}{\partial \phi} & \frac{\partial f_2}{\partial b_{1_p}} & \frac{\partial f_2}{\partial b_{1_q}} & \frac{\partial f_2}{\partial b_{1_r}} \\ \frac{\partial f_3}{\partial \psi} & \frac{\partial f_3}{\partial \theta} & \frac{\partial f_3}{\partial \phi} & \frac{\partial f_3}{\partial b_{1_p}} & \frac{\partial f_3}{\partial b_{1_q}} & \frac{\partial f_3}{\partial b_{1_r}} \\ 0 & 0 & 0 & 0 & 0 & 0 \\ 0 & 0 & 0 & 0 & 0 & 0 \\ 0 & 0 & 0 & 0 & 0 & 0 \end{bmatrix} \tag{47}$$

where, the functions $f_1,\ f_2,\ f_3$ are given by

$$\begin{aligned} f_1 &= q\left(\frac{s\phi}{c\theta}\right) + r\left(\frac{c\phi}{c\theta}\right) + b_{1_q}\left(\frac{s\phi}{c\theta}\right) + b_{1_r}\left(\frac{c\phi}{c\theta}\right) \\ f_2 &= qc\phi - rs\phi + b_{1_q}c\phi - b_{1_r}s\phi \\ f_3 &= p + q\ s\phi\ t\theta + r\ c\phi\ t\theta + b_{1_p} + b_{1_q}s\phi\ t\theta + b_{1_r}c\phi\ t\theta \end{aligned} \tag{48}$$

Thus, taking the partial derivatives of $f_1,\ f_2,\ f_3$ in Eq. (48) with respect to the state vector $\mathbf{x}(t) = \begin{bmatrix} \psi & \theta & \phi & b_{1_p} & b_{1_q} & b_{1_r} \end{bmatrix}^T$, results in

$$\frac{\partial \mathbf{f}(\mathbf{x})}{\partial \mathbf{x}} = \begin{bmatrix} 0 & \frac{s\theta g_\phi}{c^2\theta} & \frac{g'_\phi}{c\theta} & 0 & \frac{s\phi}{c\theta} & \frac{c\phi}{c\theta} \\ 0 & 0 & -g_\phi & 0 & c\phi & -s\phi \\ 0 & \frac{g_\phi}{c^2\theta} & \frac{s\theta g'_\phi}{c\theta} & 1 & s\phi t\theta & c\phi t\theta \\ 0 & 0 & 0 & 0 & 0 & 0 \\ 0 & 0 & 0 & 0 & 0 & 0 \\ 0 & 0 & 0 & 0 & 0 & 0 \end{bmatrix} \tag{49}$$

where, $g_\phi = s\phi\left(q + b_{1_q}\right) + c\phi\left(r + b_{1_r}\right)$ and $g'_\phi = \frac{\partial g_\phi}{\partial \phi} = c\phi\left(q + b_{1_q}\right) - s\phi\left(r + b_{1_r}\right)$. Furthermore, evaluating the matrix in Eq. (49) at $\hat{\mathbf{x}} = \begin{bmatrix} \hat{\psi} & \hat{\theta} & \hat{\phi} & \hat{b}_{1_p} & \hat{b}_{1_q} & \hat{b}_{1_r} \end{bmatrix}^T$ leads to the matrix $F(t)$ given by

$$F(t) = \left.\frac{\partial \mathbf{f}(\mathbf{x})}{\partial \mathbf{x}}\right|_{\mathbf{x}=\hat{\mathbf{x}}} = \begin{bmatrix} 0 & \frac{s\hat{\theta}\hat{g}_\phi}{c^2\hat{\theta}} & \frac{\hat{g}'_\phi}{c\hat{\theta}} & 0 & \frac{s\hat{\phi}}{c\hat{\theta}} & \frac{c\hat{\phi}}{c\hat{\theta}} \\ 0 & 0 & -\hat{g}_\phi & 0 & c\hat{\phi} & -s\hat{\phi} \\ 0 & \frac{\hat{g}_\phi}{c^2\hat{\theta}} & \frac{s\hat{\theta}g'_\phi}{c\hat{\theta}} & 1 & s\hat{\phi}t\hat{\theta} & c\hat{\phi}t\hat{\theta} \\ 0 & 0 & 0 & 0 & 0 & 0 \\ 0 & 0 & 0 & 0 & 0 & 0 \\ 0 & 0 & 0 & 0 & 0 & 0 \end{bmatrix} \tag{50}$$

where, $\hat{g}_\phi = s\hat{\phi}\left(q^*_m + \hat{b}_{1_q}\right) + c\hat{\phi}\left(r^*_m + \hat{b}_{1_r}\right)$ and $\hat{g}'_\phi = \left.\frac{\partial g_\phi}{\partial \phi}\right|_{\hat{\phi},\hat{b}_{1_q},\hat{b}_{1_r}} = c\hat{\phi}\left(q^*_m + \hat{b}_{1_q}\right) - s\hat{\phi}\left(r^*_m + \hat{b}_{1_r}\right)$. The process noise gain matrix Γ from Eq. (4) is given by

$$\Gamma(t) = \begin{bmatrix} 0 & \frac{s_{\hat{\phi}}}{c_{\hat{\phi}}} & \frac{c_{\hat{\phi}}}{c_{\hat{\theta}}} & 0 & 0 & 0 \\ 0 & c_{\hat{\phi}} & -s_{\hat{\phi}} & 0 & 0 & 0 \\ 1 & \frac{s_{\hat{\phi}}s_{\hat{\theta}}}{c_{\hat{\theta}}} & \frac{c_{\hat{\phi}}s_{\hat{\theta}}}{c_{\hat{\theta}}} & 0 & 0 & 0 \\ 0 & 0 & 0 & 1 & 0 & 0 \\ 0 & 0 & 0 & 0 & 1 & 0 \\ 0 & 0 & 0 & 0 & 0 & 1 \end{bmatrix} \tag{51}$$

ErKF System Matrix

The continuous-time system matrix $F(\hat{\mathbf{x}}(t))$ from Eq. (25) is obtained by perturbing each state variable of Eq. (40). Thus the perturbed variables are $\psi + \delta\psi$, $\theta + \delta\theta$, $\phi + \delta\phi$, $b_{1_p} + \delta b_{1_p}$, $b_{1_q} + \delta b_{1_q}$ and $b_{1_r} + \delta b_{1_r}$. Furthermore, the sine and cosine expansions of the perturbed attitude variables $(\phi,\ \theta)$ result in

$$\begin{aligned} \sin(\phi + \delta\phi) &= \sin(\phi)\cos(\delta\phi) + \sin(\delta\phi)\cos(\phi) \\ \cos(\phi + \delta\phi) &= \cos(\phi)\cos(\delta\phi) - \sin(\delta\phi)\sin(\phi) \\ \cos(\theta + \delta\theta) &= \cos(\theta)\cos(\delta\theta) - \sin(\delta\theta)\sin(\theta) \end{aligned} \tag{52}$$

and with small angle approximation, $\sin(\delta\theta) = 0,\ \sin(\delta\phi) = 0$ and $\cos(\delta\theta) = 1,\ \cos(\delta\phi) = 1$. The $F(t)$ matrix obtained via perturbation turns out to have the same structure as shown in Eq. (50). The process noise gain matrix Γ has the same expression as given in Eq. (51).

Acknowledgments

The authors express their gratitude towards Shri. Shyam Chetty, Scientist 'H' & Divisional Head, Flight Mechanics and Control Division (FMCD), National Aerospace Laboratories (NAL), Bangalore, India for motivating and providing the necessary support for this research effort. The authors would also like to acknowledge Dr. Abhay A. Pashilkar, Scientist 'E-II' & Group Head, Flight Simulation at FMCD, NAL, Bangalore, for providing insightful comments that enhanced the flow of the manuscript.

References

[1]D. G. Luenberger, "Observing the state of a linear system", *IEEE Trans. Milit. Electr.*, 8:74, 1963.

[2]N. Wiener, The extrapolation, interpolation and smoothing of stationary time series, John Wiley & Sons, Inc., New York, 1949.

[3]R. A Singer and P. A. Frost, "On the relative performance of the Kalman and Wiener filters", *IEEE Transactions on Automatic Control*, 17(4):390 - 394, August, 1969.

[4]R. E. Kalman, "A New Approach to Linear Filtering and Prediction Problems", *Transactions of the ASME - Journal of Basic Engineering*, 82 (Series D): 35-45, 1960.

[5]R. E. Kalman and R. S. Bucy, "New Results in Linear Filtering and Prediction Theory", *Transactions of the ASME - Journal of Basic Engineering*, 83 (Series D): 95-108, 1961.

[6]Robert Brown and Patrick Hwang, Introduction to Random Signals and Applied Kalman Filtering, John Wiley and Sons, Inc., 1992.

[7]C. Hutchinson, "An example of the equivalence of the Kalman and Wiener filters", *IEEE Transactions on Automatic Control*, 11(2):324, April, 1966.

[8]Nijmeijer. H and Fossen. T, "New directions in nonlinear observer design", editors, Lecture Notes in Control and Information Sciences 244. Springer Verlag, London, 1999.

[9]Fred Daum, "Nonlinear filters: beyond the Kalman filter", IEEE Aerospace and Electronic Systems Magazine, Vol. 20, No. 8, pp. 57 - 69, August 2005.

[10]P. Eykhoff, System Identification, Wiley, 1974.

[11]A. H. Jazwinski, Stochastic Processes and Filtering Theory, New York, Academic, 1970.

[12]Hisashi Tanizaki, Nonlinear Filters: Estimation and Applications, 2^{nd} Edition, Springer-Verlag, Berlin 1996.

[13]H. Cox, "Estimation of State Variables Via Dynamic Programming", *In the Proceedings of the Joint Automatic Control Conference*, pp. 376 - 381, Stanford, CA, June 1964.

[14]W.H. Fleming and S.K. Mitter, "Optimal Control and Nonlinear Filtering for Nondegenerate Diffusion Processes", *Stochastics*, Vol. 8, pp. 63 - 77, 1982.

[15]M.G. Safonov and M. Athans, "Robustness and Computational Aspects of Nonlinear Stochastic Estimators and Regulators", *IEEE Transactions on Automatic Control*, Vol. AC - 23, pp. 717 - 726, August 1978.

[16]A. Gelb, Applied Optimal Estimation, Cambridge, MA: MIT Press, 1984.

[17]H. Sorenson, "Guest editorial: On applications of Kalman filtering", *IEEE Transactions on Automatic Control*, Vol. AC-28, No. 3, pp. 254 - 255, March 1983.

[18]Jeffrey H. Ahrens and Hassan K. Khalil, "Closed-Loop Behavior of a Class of Nonlinear Systems Under EKF - Based Control", *IEEE Transactions On Automatic Control*, Vol. 52, No. 3, March 2007.

[19]J. S. Baras, A. Bensoussan, and M. R. James, "Dynamic observers as asymptotic limits of recursive filters: Special cases", *SIAM Journal of Applied Mathematics*, Vol. 48, No. 5, pp. 1147 - 1158, 1988.

[20]O. Hijab, Minimum Energy Estimation, Ph.D Dissertation, University of California, Berkeley, CA, December 1980.

[21]Daniel B. Grunberg and Michael Athans, "Guaranteed Properties Of The Extended Kalman Filter", *MIT Laboratory for Information and Decision Systems*, (supported by the NASA Ames and Langley Research Centers under grant NASA NAG 2 - 297), LIDS - P - 1 724, December 1974.

[22]M. Boutayeb and D. Aubry, "A strong tracking extended Kalman observer for nonlinear discrete-time systems", *IEEE Transactions on Automatic Control*, Vol. 44, No. 8, pp. 1550 - 1556, August 1999.

[23]M. Boutayeb, H. Rafaralahy, and M. Darouach, "Convergence analysis of the extended Kalman filter used as an observer for nonlinear deterministic discrete-time systems", *IEEE Transactions on Automatic Control*, Vol. 42, No. 4, pp. 581 - 586, April 1997.

[24]F. Deza, E. Busvelle, J. P. Gauthier, and D. Rakotopara, "High gain estimation for nonlinear systems", *System and Control Letters*, Vol. 18, pp. 295 - 299, 1992.

[25]Augustin Banyaga, The structure of classical diffeomorphism groups, Mathematics and its Applications, 400, Kluwer Academic, 1997.

[26]K. Reif, F. Sonnemann, and R. Unbehauen, "An EKF-based nonlinear observer with a prescribed degree of stability", *Automatica*, Vol. 34, pp. 1119 - 1123, 1998.

[27]Y. K. Song and J. W. Grizzle, "The extended Kalman filter as a local asymptotic observer for nonlinear discrete-time systems", *Journal of Math Systems, Estimation and Control*, Vol. 5, pp. 59 - 78, 1995.

[28]J.P. Gauthier, H. Hammouri and S. Othman, "A simple observer for nonlinear systems - application to bioreactors", *IEEE Transactions on Automatic Control*.

[29]F. Viel, E. Busvelle, and J. P. Gauthier, "Stability of polymerization reactors using I/O linearization and a high-gain observer", *Automatica*, Vol. 31, pp. 971 - 984, 1995.

[30]A. R. Teel and J. Hespanha, "Examples of GES systems that can be driven to infinity by arbitrarily small additive decaying exponentials", *IEEE Transactions on Automatic Control*, Vol. 49, No. 8, pp. 1407 - 1410, August 2004.

[31]K. Reif and R. Unbehauen, "The extended Kalman filter as an exponential observer for nonlinear systems", *IEEE Transactions on Signal Processing*, Vol. 47, No. 8, pp. 23242328, August 1999.

[32]T. L. Song and J. L. Speyer, "A Stochastic Analysis of a Modified Gain EKF with Applications to Estimation with Bearings Only Measurements", *IEEE Transactions on Automatic Control*, Vol. AC - 30, No. 10, October 1985.

[33]H. J. SusSmann and P. V. Kokotovic, "The Peaking Phenomenon and the Global Stabilization of Nonlinear Systems", *IEEE Transactions On Automatic Control*, Vol. 36, No. 4, April 1991.

[34]M. Athans, R.P. Wishner, A. Bertolini, "Suboptimal State Estimation for Continuous Time Nonlinear Systems from Discrete Noisy Measurements", *IEEE Transactions on Automatic Control*, Vol. AC - 13, October 1968.

[35]Venkatesh K. Madyastha, Vijaysai Prasad and Venkatram Mahendraker, "Reduced Order Model Monitoring and Control of a Membrane Bioreactor System via Delayed Measurements", *In the Proceedings of the* 7^{th} *IWA Leading-Edge Conference on Water and Wastewater Technologies*, June 2 - 4, Phoenix, Arizona, USA, 2010.

[36]Venkatesh Madyastha, Vijaysai Prasad and Venkatram Mahendraker, "Reduced Order Model Monitoring and Control of a Membrane Bioreactor System via Delayed Measurements", Water Science and Technology, 2010.

[37]V. Madyastha and VijaySai Prasad, "Joint State & Parameter Estimation for a Membrane Bio Reactor System", 5^{th} International Symposium on Design, Operation & Control of Chemical Processes, PSE Asia, 2010.

[38]H.J. Kushner, "Nonlinear Filtering: The Exact Dynamical Equation Satisfied by the Conditional Mode", *IEEE Transactions on Automatic Control*, Vol. AC-12, No. 3, pp. 262 - 267, June 1967.

[39]V. Madyastha and A. Calise, "An Adaptive Filtering Approach to Target Tracking", *In the Proceedings of the American Controls Conference*, pp. 1269 - 1274, June 8 - 10, Portland, USA, 2005.

[40]N. Hovakimyan, A. Calise and V. Madyastha, "An Augmenting Adaptive Observer Design Methodology for Nonlinear Processes", IEEE Conference on Decision and Control, December 2002.

[41]R. K. Mehra, "A comparison of several nonlinear filters from reentry vehicle tracking", *IEEE Transactions on Automatic Control*, Vol. 16, No. 4, pp. 307 - 319, August 1971.

[42]V. C. Ravindra, Y. Bar-Shalom, and P. Willett, "Projectile identification and impact point prediction", *IEEE Transactions on Aerospace and Electronic Systems*, Vol. 46, No. 4, pp. 2004 - 2021, October 2010.

[43]X. Rong-Li and V. Jilkov, "Survey of maneuvering target tracking. Part II: Motion models of ballistic and space targets", *IEEE Transactions on Aerospace and Electronic Systems*, Vol. 46, No. 1, pp. 96 - 119, January 2010.

[44]Jonghyuk Kim and Salah Sukkarieh, "Autonomous airborne navigation in unknown terrain environments", *IEEE Transactions on Aerospace and Electronic Systems*, Vol. 40, No. 3, pp. 1031 - 1045, 2005.

[45]D. J. Spero and R. A. Jarvis, "A New Solution to the Simultaneous Localisation and Map Building (SLAM) Problem", *Technical Report MECSE-27-2005*, Monash University, July 2004.

[46]S. I. Roumeliotis, G. S. Sukhatme, and G. A. Bekey, "Circumventing dynamic modeling: evaluation of the error-state Kalman filter applied to mobile robot localization", in *Proceedings of the 1999 IEEE International Conference on Robot Localization*, pp. 1656 - 1663, Detroit, Michigan, May 1999.

[47]Demoz Gebre-Egziabher, "Design and Performance Analysis of a Low Cost Aided Dead Reckoning Navigator", PhD Dissertation, Department of Aeronautics and Astronautics, Stanford University, Stanford, CA, Dec - 2003.

[48]D. H. Titterton and J. L. Weston, *Strapdown Inertial Navigation Technology*, IEE, 1997.

[49]B. Barshan and H. F. Durrant-Whyte, "Inertial navigation systems for mobile robots", *IEEE Transactions on Robotics and Automation*, Vol. 11, No. 3, pp. 328 - 342, June 1995.

[50]Demoz Gebre-Egziabher, Roger C. Hayward and J. David Powell,"Design of Multi-Sensor Attitude Determination Systems", *IEEE Transactions on Aerospace and Electronic Systems*, Vol. 40, No. 2, pp. 627-649, April, 2004.

[51]P. Setoodeh, A. Khayatian, and E. Farjah, "Attitude estimation by separate-bias Kalman filer-based data fusion", *The Journal of Navigation*, Vol. 57, pp. 261 - 273, 2004.

[52]M. Koifman and S. J. Merhav, "Autonomously aided strapdown attitude reference system", *Journal of Guidance and Control*, Vol. 14, pp. 1164 - 1172, 1990.

[53]Weidong Ding, J. Wang and Chris Rizos, "Stochastic modelling strategies in GPS/INS data fusion process", *International Global Navigation Satellite Systems Society, IGNSS Symposium*, Gold Coast, Australia, 2006.

[54]Mohinder S. Grewal and Angus P. Andrews, Kalman Filtering: Theory and Practice, Prentice Hall, USA, 1993.

[55]O. S. Salychev, Applied Inertial Navigation Problems and Solutions, BMSTU Press, Moscow, 2004.

[56]Alberto Isidori, Nonlinear Control Systems, Springer, Berlin, 1995.

[57]Y. Bar-Shalom, X. Rong Li and T. Kirubarajan, *Estimation with Applications to Tracking and Navigation*, Wiley-Interscience, 2003.

[58]Roger C. Hayward, Demoz Gebre-Egziabher, M. Schwall, J. David Powell, and J. Wilson, "Inertially Aided GPS Based Attitude Heading Reference System (AHRS) for General Aviation Aircraft", *In the Proceedings of the Institute of Navigation ION-GPS Conference*, pp. 1415 - 1424, 1997.

[59]Demoz Gebre-Egziabher, Roger C. Hayward, and J. David Powell, "A Low Cost GPS/Inertial Attitude Heading Reference System (AHRS) for General Aviation Applications", *In the Proceedings of the IEEE Position Location and Navigation Symposium, PLANS*, pp. 518 - 525, 1998.

[60]Roger C. Hayward, A. Marchick, and J. David Powell, "Single Baseline GPS Based Attitude Heading Reference System (AHRS) for Aircraft Applications", *In the Proceedings of the American Control Conference*, San Diego, CA, 1999.

[61]Venkatesh K. Madyastha, Vishal C. Ravindra and Girija Gopalratnam, "Air Vehicle Reference Frames, Flight Angles and Onboard Sensors", *Project Document, PD FC - 1010 (D-1-144)*, Flight Mechanics & Controls Division, National Aerospace Laboratories, December 2010.

[62]Sergey Edward Lyshevski, MEMS and NEMS: Systems, Devices and Structures, CRC Press, 2002.

[63]Sergey Edward Lyshevski, Nano- and Micro-Electromechanical Systems: Fundamentals of Micro- and Nano- Engineering, CRC Press, Boca Raton, Florida, 1999.

[64]Vishal C. Ravindra, Venkatesh K. Madyastha and Girija Gopalaratnam, "Real Micro Air Vehicle Flight Test Data Analysis to Obtain MEMS Inertial Sensor Error Characteristics", *Technical Report*, Flight Mechanics & Controls Division, National Aerospace Laboratories, 2010.

[65]The Flight Dynamics & Control Toolbox, `http://92.254.81.198/index.html`.

[66]Aerospace Blockset, *Mathworks*, `www.mathworks.com/help/toolbox/aeroblks/drydenwindturbulencemodelcontinuous.html`.

[67]Marc Rauw, "FDC1.2 - A SIMULINK toolbox for flight dynamics and control analysis", *Technical Report*, May, 2001.

[68]Bernard Etkin and Lloyd Duff Reid, Dynamics of Flight Stability and Control, 3^{rd} Edition, John Wiley and Sons, Inc., 1996.

[69]Jan Roskam, Airplane Flight Dynamics and Automatic Flight Controls - Part I, DARcorporation (Design, Analysis and Research Corporation), 2001.

[70]Mohinder S. Grewal, Lawrence R. Weill and Angus P. Andrews, Global Positioning Systems, Inertial Navigation and Integration, John Wiley and Sons, Inc., 2001.

[71]Jonghyuk Kim and Salah Sukkarieh, "SLAM aided GPS/INS Navigation in GPS Denied and Unknown Environments", International Symposium on GNSS/GPS, Sydney, Australia, December 2004.

[72]H. L. Van Trees, Detection, Estimation and Modulation Theory, John Wiley & Sons, 1968.

[73]R. Beard, D. Kingston, M. Quigley, D. Snyder, R. Christiansen, W. Johnson, T. McLain, M. Goodrich, "Autonomous Vehicle Technologies for Small Fixed Wing UAVs", *AIAA Journal of Aerospace Computing, Information, and Communication*, Vol. 2, No. 1, pp. 92-98, Jan. 2005.